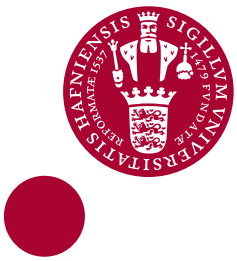

Plant Traits are Key Determinants in Buffering the Meteorological Sensitivity of Net Carbon Exchanges of Arctic Tundra

Lopez-Blanco, Efren; Lund, Magnus; Christensen, Torben R.; Tamstorf, Mikkel P.; Smallman, Thomas L.; Slevin, Darren; Westergaard-Nielsen, Andreas; Hansen, Birger U.; Abermann, Jakob; Williams, Mathew

Published in:
Journal of Geophysical Research: Biogeosciences

DOI:
10.1029/2018JG004386

Publication date:
2018

Document version
Publisher's PDF, also known as Version of record

Journal of Geophysical Research: Biogeosciences

RESEARCH ARTICLE
10.1029/2018JG004386

Key Points:
- We calibrated and validated an ecosystem model using field data to predict carbon dynamics over 8 years in West Greenland tundra
- Similar meteorological sensitivity of GPP and R_{eco} leads to buffered NEE
- Plant traits control the compensatory effect observed (and estimated) between gross primary production and ecosystem respiration

Supporting Information:
- Supporting Information S1

Correspondence to:
E. López-Blanco,
elb@bios.au.dk

Citation:
López-Blanco, E., Lund, M., Christensen, T. R., Tamstorf, M. P., Smallman, T. L., Slevin, D., et al. (2018). Plant traits are key determinants in buffering the meteorological sensitivity of net carbon exchanges of Arctic tundra. *Journal of Geophysical Research: Biogeosciences*, *123*, 2675–2694. https://doi.org/10.1029/2018JG004386

Received 9 JAN 2018
Accepted 24 JUL 2018
Accepted article online 30 JUL 2018
Published online 4 SEP 2018

Plant Traits are Key Determinants in Buffering the Meteorological Sensitivity of Net Carbon Exchanges of Arctic Tundra

Efrén López-Blanco[1,2], Magnus Lund[1], Torben R. Christensen[1,3], Mikkel P. Tamstorf[1], Thomas L. Smallman[2], Darren Slevin[2], Andreas Westergaard-Nielsen[4], Birger U. Hansen[4], Jakob Abermann[5], and Mathew Williams[2]

[1]Department of Bioscience, Arctic Research Center, Aarhus University, Roskilde, Denmark, [2]School of GeoSciences, University of Edinburgh, Edinburgh, UK, [3]Department of Physical Geography and Ecosystem Science, Lund University, Lund, Sweden, [4]Center for Permafrost (CENPERM), Department of Geosciences and Natural Resource Management, University of Copenhagen, Copenhagen, Denmark, [5]Asiaq, Greenland Survey, Nuuk, Greenland

Abstract The climate sensitivity of carbon (C) cycling in Arctic terrestrial ecosystems is a major unknown in the Earth system. There is a lack of knowledge about the mechanisms that drive the interactions between photosynthesis, respiration, and changes in C stocks across full annual cycles in Arctic tundra. We use a calibrated and validated model (soil-plant-atmosphere; SPA) to estimate net ecosystem exchange (NEE), gross primary production (GPP), ecosystem respiration (R_{eco}), and internal C processing across eight full years. SPA's carbon flux estimates are validated with observational data obtained from the Greenland Ecosystem Monitoring program in West Greenland tundra. Overall, the model explained 73%, 73%, and 50% of the variance in NEE, GPP, and R_{eco}, respectively, and 85% of the plant greenness variation. Flux data highlighted the insensitivity of growing season NEE to interannual meteorological variability, due to compensatory responses of photosynthesis and ecosystem respiration. In this modelling study, we show that this NEE buffering is the case also for full annual cycles. We show through a sensitivity analysis that plant traits related to nitrogen are likely key determinants in the compensatory response, through simulated links to photosynthesis and plant respiration. Interestingly, we found a similar temperature sensitivity of the trait-flux couplings for GPP and R_{eco}, suggesting that plant traits drive the stabilization of NEE. Further, model analysis indicated that wintertime periods decreased the C sink by 60%, mostly driven by litter heterotrophic respiration. This result emphasizes the importance of wintertime periods and allows a more comprehensive understanding of full annual C dynamics.

1. Introduction

The Arctic tundra, an important element of the global carbon (C) cycle (AMAP, 2017; Hugelius et al., 2014; McGuire et al., 2009; Tarnocai et al., 2009; Williams & Rastetter, 1999), is expected to experience changes in the current global warming context (ACIA, 2005; AMAP, 2017; Callaghan et al., 2012; Christensen et al., 2007; Grøndahl et al., 2008; Meltofte et al., 2008; Serreze & Barry, 2011). The likely increase of future temperature, precipitation, and growing season length (Arctic Climate Impact Assessment, 2005; Bintanja & Andry, 2017; IPCC, 2013) may have multiple effects on CO_2 exchange. Increases in plant productivity are expected in response to rising temperatures (Street et al., 2013), under joint warmer and wetter conditions (López-Blanco et al., 2017), or with earlier and longer growing seasons (Aurela et al., 2004; Black et al., 2000; Groendahl et al., 2007). These gains may be counterbalanced by C losses associated with microbial decomposition of soil organic matter during early winter (Commane et al., 2017; Zona et al., 2016) but also during following summer (Helfter et al., 2015; Lund et al., 2012), drought stress on plant photosynthesis under warmer conditions (Goetz et al., 2005; Hanis et al., 2015), higher rates of microbial oxidation of soil organic matter associated with warmer temperatures (Webb et al., 2016), decreases in photosynthesis due to biological disturbances (Heliasz et al., 2011; López-Blanco et al., 2017; Lund et al., 2017), permafrost thaw (Koven et al., 2011; Schuur et al., 2015), or severely burned landscapes (Rocha & Shaver, 2011). Minor variations in relation to these processes can lead to changes in ecosystem C sink functioning.

It is still a key challenge to understand the interannual variation in net ecosystem exchange (NEE) between the Arctic tundra and the atmosphere due to the large uncertainties between photosynthesis and respiration interactions (McGuire et al., 2012), and how these gross fluxes connect with C storage in vegetation and soil. The task is challenging because of insufficient coverage of measurement sites in the Arctic, particularly across annual cycles. The extreme conditions and remoteness of the Arctic (Kwon et al., 2006; Lafleur et al., 2012; McGuire et al., 2012; Poyatos et al., 2013; van der Molen et al., 2007; Westergaard-Nielsen et al., 2013), but also instrument failures, make automatic and continuous measurements difficult, especially during wintertime (Lund et al., 2012). Frequent gaps in data sets, and the inevitable bias attached to their gap filling (Falge et al., 2001; Moffat et al., 2007; Papale et al., 2006), complicate subsequent analysis because of increased uncertainty. The analysis of the annual impact of driving variables on C fluxes becomes problematic without year-round data (Grøndahl et al., 2008; López-Blanco et al., 2017; van der Molen et al., 2007), and the discussion of C source/sink dynamics is compromised without taking into account nongrowing season processes (Aurela et al., 2004; Commane et al., 2017; Zona et al., 2016).

The process-based understanding of the mechanisms driving the interplay between NEE's competing processes are not yet fully understood. Likewise, there is a lack of knowledge about each of the sub-components contributing to the respiratory losses during both the growing season and the wintertime periods (Hobbie et al., 2000). NEE is usually separated into its two key processes: photosynthesis (gross primary production [GPP]) and ecosystem respiration (R_{eco}) (Lasslop et al., 2010; Reichstein et al., 2005). Similarly, the respiratory loss splits between autotrophic respiration (R_a; the sum of growth [R_g] and maintenance [R_m] respiration from leaves, stems, and roots) and heterotrophic respiration (R_h; litter and soil organic matter decomposition) (Waring & Schlesinger, 1985). These components change not only within seasons but also from year to year, in response to both biotic and abiotic drivers, and can vary among tissue types (Hopkins et al., 2013; Reich et al., 2008; Tjoelker et al., 2001; Waring & Schlesinger, 1985). The decomposition of gross fluxes in Arctic ecosystems remains unquantified at such high levels of complexity (McGuire et al., 2012). Furthermore, terrestrial ecosystem models frequently assume fixed values of carbon use efficiency (CUE), the proportion of GPP allocated to growth, usually based on a predefined fraction of GPP respired as R_a. CUE needs to be sensitive to biological states (such as tissue N concentration), and environmental conditions (Bradford & Crowther, 2013). Without accurate estimates of current carbon fluxes from the Arctic, predicting the response of these systems to global change is challenging (Hobbie et al., 2000). Therefore, studies on C storage and turnover controls are needed and special attention must be paid to dynamic systems including positive feedbacks, which will ultimately lead into a more comprehensive picture of the Arctic ecosystem-atmosphere interactions.

We have previously found that eddy covariance (EC) derived ecosystem flux data suggest an insensitivity to meteorology of growing season NEE across interannual variability (López-Blanco et al., 2017). This insensitivity was despite large variability in temperature and precipitation through the growing seasons. The net CO_2 budget was surprisingly stable compared to the magnitude of variations in GPP and R_{eco} inferred from the eddy flux data. We concluded that the meteorological sensitivity of photosynthesis and ecosystem respiration were similar, and hence compensatory, but we could not explain the causes. This research led to two key questions. First, is this meteorological buffering of NEE also the case over full annual cycles? Second, what determines the meteorological insensitivity of NEE? We hypothesize that plant traits, particularly foliar N, are critical in causing the similar meteorological sensitivities of photosynthesis and respiration. Foliar N mediates both photosynthesis and a major fraction of autotrophic respiration.

In this study we applied a process-based terrestrial ecosystem model, combined with extensive field measurements to simulate year-round C fluxes (and hence CUE) and C stocks in plants and soils, and address these questions. We used the modified, calibrated and validated soil-plant-atmosphere (SPA) model (Williams et al., 1996) to report independent predictions from observational data measured by the Greenland Ecosystem Monitoring (GEM) program (http://g-e-m.dk/) in West Greenland tundra (64°N), across 8 years between 2008 and 2015. The Kobbefjord site is currently the southernmost station in the low Arctic Western Greenland equipped for measurement of terrestrial CO_2 exchange. Our aim using this data-model framework was to quantify (1) how realistically the SPA model can simulate growing season C fluxes in Arctic tundra, and the sensitivity of key parameters in calibrating the model; (2) the role of the winter period on the full annual-cycle C balance, to determine if NEE is insensitive to meteorology over full annual cycles;

and (3) untangling the effects of competing ecosystem processes and their links to plant traits, testing the hypothesis that plant N and vegetation properties are important controls on the tight link between GPP and R_{eco}, through the role of N in metabolic processes. Ultimately, discrepancies between model and data emerging from these questions can provide helpful information about knowledge gaps and ecological indicators not previously detected from field observations, emphasizing the unique synergy that models and data are capable of bringing together.

2. Materials and Methods

2.1. Site Description

Kobbefjord is a valley system located in the low Arctic in Western Greenland (64°07′N; 51°21′W). The study area is located ~20 km from Nuuk, Greenland's capital, and has been subjected to extensive environmental research activities since 2007 within the Nuuk Ecological Research Operations program under the auspices of the GEM program (http://g-e-m.dk/). The Kobbefjord area presents high meteorological variability from year to year, with a mean annual air temperature of −0.4 °C (ranging between −1.7 °C in 2011 and 3.4 °C in 2010) and a total annual precipitation of about 862 mm between 2008 and 2015 (López-Blanco et al., 2017). There is no continuous permafrost at the site and the annual variation of the maximum snow depth observed in our measurement period was 0.4 to 1.4 m. The water table in Kobbefjord fluctuated between +0.53 cm (sign of water abundance at the end of the growing season) and −18 cm (sign of water stress at the peak of the growing season) in the 2010–2015 period. However, no apparent water limitation on C dynamics has been found in the ecosystem, likely resistant to drought due to the water from the surroundings (López-Blanco et al., 2017). The vegetation in the key study site—a fen ecosystem—is dominated by *Eriophorum angustifolium* and *Scirpus caespitosus*, and it is surrounded by heath species such as *Empetrum nigrum*, *Vaccinium uliginosum*, and copse species as *S. glauca* and *Eriophorum angustifolium* (Bay et al., 2008). For more information, see López-Blanco et al., 2017.

2.2. Field Observations: Model Forcing, Calibration, and Validation

First, this research used data from the meteorological towers located at the Kobbefjord site during the 2008–2015 period to drive the SPA model to estimate C fluxes and stocks. The ancillary data (air temperature [T_{air}; °C], vapor pressure deficit [VPD; kPa] shortwave radiation [SWR; W/m^2], photosynthetic active radiation [PAR; μmol m^{-2} s^{-1}], total precipitation [P; mm], and snow coverage [S; %]; Figure S1; hereafter, S denotes additional information) presented gaps no larger than 0.3% for T_{air} and VPD and 10% for SWR, PAR, and P due to poor weather and instrument malfunction. Since the model requires gap-filled inputs, we gap filled the meteorological data using daily ERA-Interim reanalysis (Dee et al., 2011) products (T_{air}, dew point temperature [T_{dp}], P and SWR). The T_{air} and T_{dp} consist of data at 00Z, 06Z, 12Z, and 18Z (instantaneous values). P and SWR consist of data at 00Z and 12Z (totals for the previous 12 hr). We used a weather generator code (full description can be found in Text S1) to apply a diurnal cycle to the T_{air} and SWR variables. PAR was calculated to be twice the SWR. Finally, we resampled the data set from hourly to half-hour temporal resolution for the SPA model.

Further, we performed a 4-week fieldwork campaign between June and July 2015 to obtain site-specific measurements on local aboveground vegetation and soil structure. The footprint analysis performed by Westergaard-Nielsen et al. (2013) suggested an overall contribution of fen (63.9%), heath (23.7%), copse (9.0%), and bedrock (3.4%) to the EC measurements. Therefore, we intentionally selected five plots in the fen site together with three and two more plots from the surrounding heath and copse, respectively. We sampled the aboveground vegetation from 10 plots of 10 cm × 10 cm square area, and the soil underneath at a maximum depth of 20 cm, within a 100-m radius of the location of the EC tower. The samples were collected on 12 August (1 week earlier than GPP at maximum capacity), frozen, and shipped to the laboratory. In the laboratory, we (1) separated the different tissue types by hand (i.e., leaves, stems, roots, litter, and mosses) from the aboveground biomass and roots from the soil cores, (2) measured the leaf area index (LAI) using Image J (Schneider et al., 2012), (3) dried at 70 °C until constant weight during ~48 hr, (4) weighted the resulting dry samples, (5) subsampled each stock before the carbon and nitrogen (CN) analysis, (6) finely grinded using a ball mixer at maximum frequency (25 Hz) during 2 min, and (7) measured total CN contents using a NC 2500 analyzer. After this, we calculated the leaf mass per area (LMA), total foliar nitrogen and total leaf, stem, root, and litter C content at the harvesting date (Figure S2). Stem here does not strictly refer to

woody material; it is just structural biomass that is not photosynthetic (leaves) or absorbing water/nutrients from the soil (roots). Since our aim was to simulate the observations from the fen site, only data from this ecotype was used to calibrate the vegetation parameters in the model initialization.

We manually calibrated the last 4 years of the time series (2012–2015) and then validated the initial 4 years (2008–2011) including the anomalous year 2011, ensuring that both the calibration and validation data sets do not overlap. The calibration period was specifically selected to exclude the moth outbreak in 2011 to quantify the model-data mismatch introduced by the biological disturbance, which is not represented in the model. The state variables for the earlier 4 years were calibrated based on matching to stocks the final 4 years. The calibration procedure of the model parameters used field data, values retrieved from literature and tuning of turnover rates of the C stocks (Table 1) to match the stock data for the calibration years. Moreover, we targeted NEE, GPP, R_{eco}, and LAI as key variables aiming for a defined, acceptable degree of statistical agreement. The statistical metrics we considered acceptable were (1) $R^2 \geq 0.7$ for NEE, GPP, and LAI (compared with % of Greenness) and ≥0.5 for R_{eco}; (2) RMSE ≤ 1 g C m^{-2} $year^{-1}$, and (3) mean bias ≤1 g C m^{-2} $year^{-1}$ for the simulated period for these four variables.

We used NEE data during the final 4 years for calibration, then used to testing the first 4 years. We processed, gap filled, and partitioned EC data on NEE measured during eight snow-free seasons across the 2008–2015 period. The measurement season is typically scheduled between the snow melt period in spring and the snow freeze-in period at the end of summer. The end of the snow melt period and the growing season start and length present high interannual variability (López-Blanco et al., 2017). In 2014 the EC station suffered a major instrument failure that translated in the loss of half of the growing season data. The EC tower is equipped with a closed-path infrared CO_2 and H_2O gas analyzer LI-7000 (LI-COR Inc., USA) and a 3-D sonic anemometer Gill R3-50 (Gill Instruments Ltd, UK). We processed NEE gap-filled and partitioned NEE using ReddyProc's technique (López-Blanco et al., 2017). In this study, we used the meteorological sign of convention representing uptake and release of C with negative and positive values, respectively.

Moreover, we used a daily estimate of the timing of snowmelt and freeze-in period to constrain the soil temperature during the wintertime, as well as the % of greenness to determine the phenology timing (seasonality) at a pixel level from a time-lapse camera (HP e427) located at 500 m asl. (Westergaard-Nielsen et al., 2013). We used % of greenness to constrain and validate model estimations. Percent of greenness data were used as input in the last 4 years (calibration set) to tune the decay slope after the peak of the growing season of LAI, then used as an independent test only in 2010 and 2011 due to the lack of greenness data in 2008 and 2009. The % of greenness, an index based on the three colors in a digital camera, RedGreenBlue, was computed as G/(R + G + B), which normalizes for changes in illumination. It was recently found that the physical reason for the % of greenness signal was a mix of leaf color, LAI, and the background (Keenan et al., 2014). Additionally, the seasonal greening of the vegetation was measured using a SpectroSense 2+ handheld system with two mounted sensors, which calculates the greening index (normalized difference vegetation index—NDVI) to cross check the % of greenness data from the automatic photo camera in the fen site. Measurements were made 4–5 times across snow-free periods.

2.3. Model Description

This study utilizes process-based modeling at leaf-level scale (parameterization) and canopy-level scale (prediction). The SPA model (Figure 1; Williams et al., 1996) uses a multiple canopy layer approach (up to 10 layers) linking each canopy layer independently to root accessible soil layers (up to 20 layers; Williams et al., 1996). SPA estimates ecosystem fluxes of C, water and energy coupling its leaf level C, water and energy cycles through eco-physiological principles. SPA has been already validated against EC observations in Arctic tundra (Williams et al., 2000) but also in tropical rain forest (Williams et al., 1998), temperate deciduous forests (Williams et al., 1996), or temperate evergreen forests (Williams et al., 2001). The model requires a simple set of measurable meteorological-related variables together with vegetation- and soil-related parameters, completely independent of flux data, against which the model can be compared (Williams et al., 2000). SPA uses a multilayer canopy radiative transfer scheme accounting for both sunlit and shaded leaf area (Williams et al., 1998). Photosynthesis is simulated using a detailed representation of carboxylation (Farquhar & von Caemmerer, 1982). The critical V_{cmax} and J_{max} parameters are linearly related to foliar N. Moreover, the evaporative fluxes (wet surface, soil, and transpiration) are based on the Penman-Monteith model (Jones, 1992). Photosynthesis and transpiration are linked through a stomatal optimization scheme, which aims to

Table 1
Ranking Table Listing the S-Indices (SI) for NEE, GPP, and R_{eco} Subject to the Average ±10% Change of Each of the 36 Ecosystem Parameters in SPA

Parameter	Unit	Function	Value	Source	SI-NEE	SI-GPP	SI-R_{eco}
Initial autotrophic respiration C	g C m^{-2}	IC	0	Field data	0.000	0.000	0.000
Initial foliage C	g C m^{-2}	IC	0	Field data	0.000	0.000	0.000
Root biomass to reach 50% of max depth	g m^{-2}	SS	50	Smallman et al., 2013	0.000	0.000	0.000
Turnover rate of autotrophic respiration pool	hr^{-1}	CC	0.07	Smallman et al., 2013	0.000	0.000	0.000
Water retained by canopy	mm	WC	1	Williams et al., 1996, 2000	0.000	0.000	0.000
Leaf capacitance	mmol m^{-2} leaf area MPa^{-1}	CS	4000	Smallman et al., 2013	0.004	0.000	0.001
Stem conductivity	mmol m^{-1} s^{-1} MPa^{-1}	CS	5	Smallman et al., 2013	0.008	0.002	0.002
Maximum root depth	m	SS	0.5	Smallman et al., 2013	0.015	0.000	0.002
Minimum temperature threshold	deg C	PH	10	van der Kolk et al., 2016	0.031	0.008	0.006
Minimum leaf water potential	MPa	WC	-1.5	Williams et al., 2000	0.037	0.008	0.004
Turnover rate of wood	hr^{-1}	CC	0.000008	Tuned	0.045	0.000	0.005
Precipitation that penetrates canopy	fraction	WC	0.7	Williams et al., 1996, 2000	0.048	0.000	0.006
Root resistivity	MPa s g $mmol^{-1}$	CS	20	Smallman et al., 2013	0.049	0.005	0.000
Initial wood C	g C m^{-2}	IC	70	Field data	0.070	0.000	0.008
Width of leaf	m	CS	0.02	Williams et al., 2000	0.078	0.022	0.015
GDD threshold	deg C	PH	10	Shulski and Wendler, 2007	0.092	0.021	0.014
Decomposition rate	hr^{-1}	CC	0.000004	Smallman et al., 2013	0.155	0.000	0.018
Initial labile C	g C m^{-2}	IC	13	Tuned	0.176	0.056	0.043
Turnover rate of foliage	hr^{-1}	CC	0.0029	Hobbie et al., 2000	0.324	0.084	0.058
Respiratory cost of labile transfers	fraction	CC	0.129	Smallman et al., 2013	0.373	0.058	0.023
Stomatal efficiency parameter	µmol CO_2 $mmol^{-1}$ H_2O m^{-2} s^{-1}	WC	1.007	Smallman et al., 2013	0.407	0.059	0.010
Turnover rate of fine roots	hr^{-2}	CC	0.000009	Sloan et al., 2013	0.440	0.036	0.089
Initial litter C	g C m^{-2}	IC	60	Field data	0.499	0.000	0.056
Mineralization rate of litter	hr^{-1}	CC	0.000055	Tuned	0.585	0.000	0.065
Turnover rate of labile pool	hr^{-1}	CC	0.0022	Tuned	0.629	0.131	0.075
NPP allocated to foliage	fraction	CC	0.7	Smallman et al., 2013	0.713	0.147	0.084
Fraction of leaf loss to litter	fraction	CC	0.3	Tuned	0.963	0.166	0.077
NPP allocated to roots	fraction	CC	0.7	Smallman et al., 2013	1.052	0.033	0.080
Mineralization rate of SOM	hr^{-1}	CC	0.000001	Tuned	1.259	0.000	0.140
Rate coefficient for V_{cmax}	µmol C g N^{-1} s^{-1}	PT	14	Smallman et al., 2013	1.334	0.227	0.104
Initial SOM C	g C m^{-2}	IC	4800	Hugelius et al., 2013	1.346	0.001	0.150
Initial root C	g C m^{-2}	IC	200	Field data	1.584	0.047	0.124
Average foliar nitrogen	g N m^{-2}	CS	1.61	Field data	3.154	0.916	0.667
Maximum foliar carbon stock	g C m^{-2}	CC	28	Field data	3.868	0.922	0.595
Rate coefficient for J_{max}	µmol C g N^{-1} s^{-1}	PT	36	Smallman et al., 2013	4.432	0.786	0.369
Leaf mass per area	g C m^{-2}	CS	56.27	Field data	4.546	1.137	0.769

Note. The table orders the S-indices (NEE) starting with the lowest value and increasing to the highest value. The function column classifies the parameters based on their role, that is, photosynthetic (PT), C cycle (CC), water cycle (WC), initial conditions (IC), canopy structure (CS), soil structure (SS), and phenology (PH). The colors represent how sensitive the parameter is to the response variable: green = little sensitive; red = very sensitive. A further test of the four most sensitive parameters is proposed in Figure 6 (pink highlight).

maximize C accumulation within SPA's hydraulic limitations. SPA simulates both the vertical distribution and movement of water and heat through the soil profile. A detailed overview of SPA can be found in Smallman et al. (2013). Plant phenology and carbon dynamics are simulated using a box carbon model, the Data Assimilation Linked Ecosystem Carbon model imbedded within the SPA framework, which simulates the states and dynamics of ecosystem C stocks (foliage, structural/wood carbon, fine roots, labile carbon, soil organic matter (SOM), and surface litter) (Williams et al., 2005). In SPA, the unique allocations groupings are (1) foliar allocation is a fixed fraction from NPP (Table 1; NPP allocated to foliage), dependent on growing degree day summation, restarting from the snow melt period (retrieved from the photo monitoring) and (2) stem and root allocation are dependent on a fixed fraction from NPP (Table 1; NPP

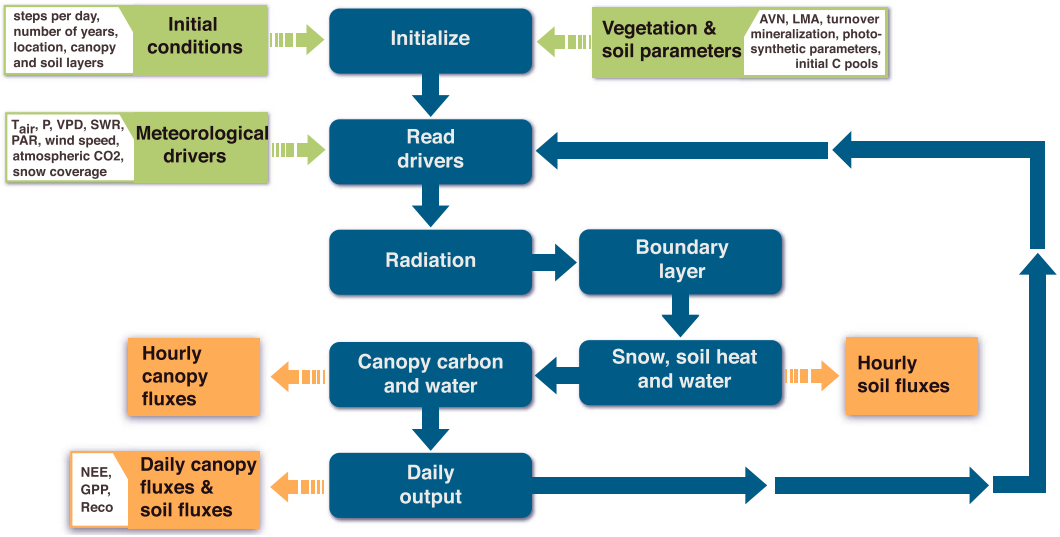

Figure 1. Schematic description of the soil-plant-atmosphere model. The blue boxes represent the key model components, while the green boxes the model inputs and the orange boxes the model outputs.

allocated to roots, while NPP allocated to stems is 1-NPP allocated to roots). The plant phenology in SPA is entirely driven by meteorological forcing unless stated otherwise. The unique turnover groupings are (1) foliar turnover, driven by a minimum temperature threshold (Table 1) and a predefined day at the end of August and (2) roots and stem represented as a constant loss fraction assuming first-order kinetics. Litter decomposition to SOM, litter mineralization ($R_{h\ litter}$) and SOM mineralization ($R_{h\ som}$) follow a similar continuous decay process with exponential temperature adjustment. Leaves and fine root mortality is directly input to the litter stock, while woody mortality is directly input to the SOM stock. Thus we assume different labilities for the dead organic C depending on tissue source. The collected data were used to parameterize and evaluate the Arctic specific branch in SPA in order to simulate the full range of biogeochemical feedbacks in West Greenland.

The model has been modified to introduce a revised C allocation approach, which separately estimates respiration associated with growth (R_g) and maintenance (R_m) respiration. Growth respiration is assumed to be a fixed fraction of C allocated to each tissue using the following equations:

$$R_{g\ leaf} = \left(GPP_{leaf}{}^{*}\ R_g\ frac\right); NPP_{leaf} = alloc_{leaf} - R_{g\ leaf} \quad (1)$$

$$R_{g\ root} = \left(GPP_{roots}{}^{*}\ R_g\ frac\right); NPP_{root} = alloc_{roots} - R_{g\ root} \quad (2)$$

$$R_{g\ stem} = \left(GPP_{stem}{}^{*}\ R_g\ frac\right); NPP_{stem} = alloc_{stem} - R_{g\ stem} \quad (3)$$

where R_g is assumed to be a fixed fraction of C allocated (alloc) to a given tissue ($R_{g\ frac}$) equivalent to 21% of NPP (Waring & Schlesinger, 1985). Further, maintenance respiration (R_m) has been calculated based on a modified version of the Reich et al. (2008) calculation in SPA, which demonstrated a strong respiration-nitrogen (N) relationship among tissue types (leaves, stems, and roots). The R_m in leaves has been calculated based on air temperature, average foliar N, leaf C per area, and LAI, only when the air temperatures >0 °C. R_m in roots was calculated based on soil temperatures at 10 cm depth, the C:N relation in roots and the root C stock, following the same freezing point limitation. Finally, a brief description of the equations showing the different components of the C fluxes related to each other is provided in the supporting information equation S1.

The snowpack thickness has a direct influence on soil temperatures and consequently on respiration processes. Therefore, we also implemented a snow cover subroutine in order to constrain soil temperature across wintertime periods. We used snow fraction information (Figure S3) recorded from the camera pointing towards the fen site (Westergaard-Nielsen et al., 2013) to inform a simplified version of the snow scheme by

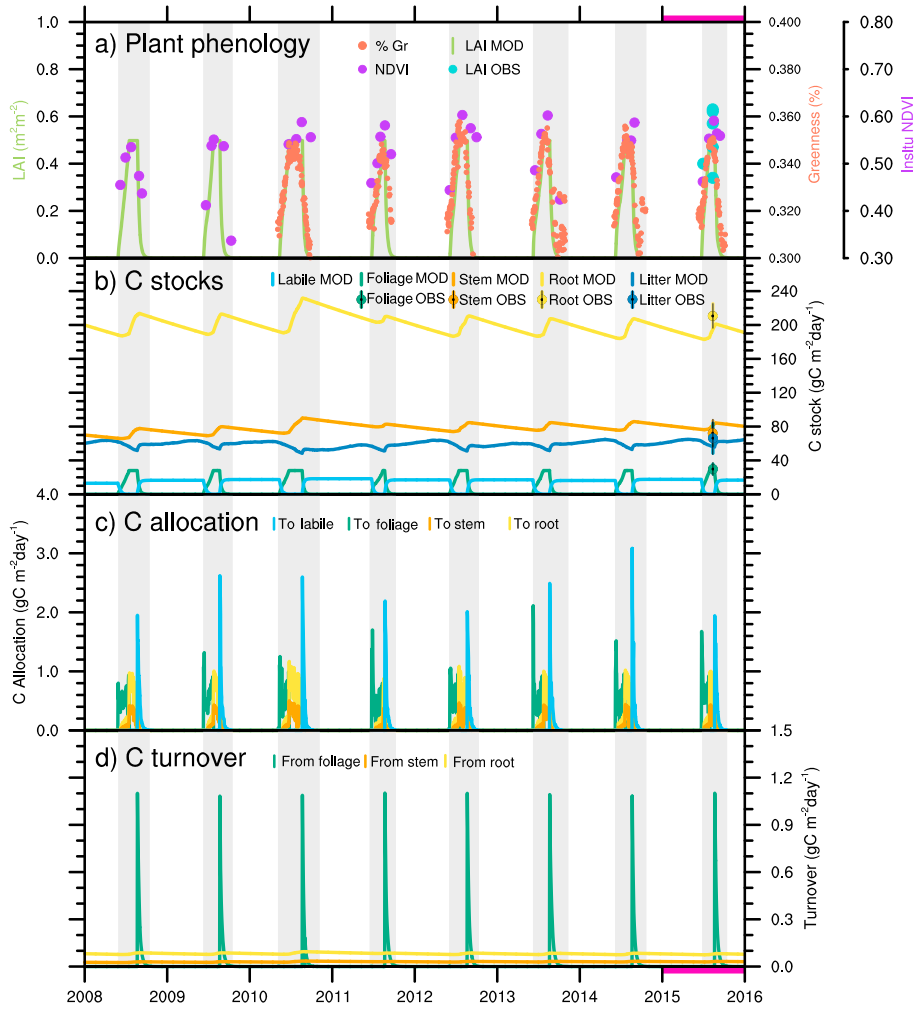

Figure 2. Time-series of observed (OBS) and predicted (MOD) plant phenology (%Gr, % of greenness; NDVI, in situ normalized difference vegetation index; LAI, leaf area index) (a) and C stocks (labile, foliage, stem, root, and litter) (b), as well as simulated C allocation (to labile, foliage, stem, and root) (c) and C turnover [from foliage, stem, and root] (d). The gray shading denotes the snow-free period reported in López-Blanco et al. (2017). The 2015 C dynamics (pink highlights) are presented in detail in Figure S5.

Essery (2015). The modified snow scheme used snow fractional cover to update the soil surface energy balance including albedo, evaporative, and sensible heat exchanges.

2.4. Sensitivity Analysis

We conducted a sensitivity analysis of the vegetation related parameters used in SPA to determine how critical each is to the estimation of NEE, GPP, and R_{eco}. By identifying how sensitive NEE, GPP and R_{eco} are to changes in each of the 36 parameters, we identify potential model limitations of the simulated C dynamics (e.g., C allocation, C turnover, phenology, and seasonality). The sensitivity analysis also helps to test the robustness of model outputs in presence of uncertainty. We first determined 36 nominal parameters values (Table 1) and confirmed that these generate reasonable model fluxes compared to the flux tower data. We decided our response variables for the sensitivity analysis as total annual NEE, GPP, and R_{eco}. In sequence, we modified each parameter ±10%. We evaluated the percentage change in the response variable. The ratio of the % change in response variable to % change in parameter is the sensitivity index (SI), such that if $|SI| > 1$ [$|SI|$ = magnitude of S], the parameter is very sensitive to the response variable; close to 0 means little sensitivity. We tested the sensitivity analysis for the entire data set and for each year independently. Additionally, we assessed the relationships between the four most sensitive parameters in the model

Table 2
Statistics of Linear Fit Between the SPA Model (Independent) and the Field Observations (Dependent) per Individual Year and for the Entire 2008–2015 Period

		Validation set					Calibration set
	Statistics	2008	2009	2010	2011	2008–2011	2012
NEE	Intercept	−0.12 (−0.16/−0.07)	−0.12 (−0.16/−0.08)	−0.23 (−0.29/−0.18)	−0.16 (−0.21/−0.1)	−0.17 (−0.19/−0.14)	−0.08 (−0.12/−0.04)
	Slope	0.66 (0.59/0.72)	0.83 (0.76/0.9)	0.63 (0.57/0.69)	0.52 (0.42/0.62)	0.65 (0.61/0.68)	0.52 (0.48/0.56)
	R^2	0.72	0.76	0.74	0.42	0.7	0.8
	RMSE	0.28	0.26	0.35	0.31	0.31	0.24
	Bias	−0.02	−0.1	−0.18	−0.28	−0.15	0.03
GPP	Intercept	0.06 (−0.06/0.18)	0.24 (0.13/0.35)	0.16 (0.01/0.31)	0.12 (−0.02/0.26)	0.15 (0.09/0.22)	0.16 (0.05/0.27)
	Slope	0.96 (0.89/1.04)	1 (0.97/1.13)	0.95 (0.88/1.03)	0.88 (0.74/1.02)	0.97 (0.93/1.01)	0.59 (0.54/0.63)
	R^2	0.82	0.8	0.79	0.51	0.77	0.84
	RMSE	0.46	0.47	0.54	0.54	0.51	0.43
	Bias	0.11	0.19	0.23	0.21	0.19	1.01
Reco	Intercept	−0.28 (−0.35/−0.2)	−0.19 (−0.23/−0.14)	−0.14 (−0.22/−0.07)	−0.29 (−0.34/−0.25)	−0.21 (−0.24/−0.18)	−0.18 (−0.25/−0.12)
	Slope	0.88 (0.79/0.97)	0.88 (0.82/0.94)	0.7 (0.63/0.77)	0.79 (0.73/0.85)	0.78 (0.74/0.81)	0.43 (0.39/0.47)
	R^2	0.52	0.72	0.55	0.66	0.59	0.56
	RMSE	0.36	0.26	0.42	0.22	0.33	0.35
	Bias	−0.37	−0.26	−0.42	−0.44	−0.37	−0.96
LAI	Intercept	—	—	0.31 (0.31/0.31)	0.32 (0.31/0.32)	0.31 (0.31/0.32)	0.32 (0.31/0.32)
	Slope	—	—	0.06 (0.06/0.07)	0.06 (0.05/0.06)	0.06 (0.06/0.06)	0.07 (0.06/0.08)
	R^2	—	—	0.90	0.75	0.83	0.88
	RMSE	—	—	0.00	0.01	0.01	0.01
	Bias	—	—	0.03	0.11	0.06	0.07

Note. The data set was divided into a calibration set (2008–2011) and a validation set (2012–2015). The presented statistics are from a model run entirely driven by environmental data, based on growing degree day summation restarted from the snow melt period and minimum temperature threshold, both calculated from soil temperatures at 10 cm depth. The parentheses represent the 95% confidence interval for the intercepts and slopes. The units for RMSE and bias are g C m^{-2} $year^{-1}$ in NEE, GPP, and R_{eco}, and m^2 m^{-2} in LAI.

against mean annual temperature. This assessment tested whether the sensitivity of both GPP and R_{eco} to plant traits is coupled or decoupled across meteorological variation. We hypothesized that the metabolic processes (photosynthesis and autotrophic respiration) that are coupled by plant traits in the model would have similar temperature sensitivity.

3. Results

The SPA model performed well in simulating the observed plant phenology (Figure 2a and Table 2) and C fluxes (Figure 3 and Table 2), tracking the variations observed across multiseasonal and multiannual periods. We modelled full annual C dynamics despite the lack of field observations during winter by implementing a snow cover subroutine constrained by snow fraction data (Figure S3). The data constraint improved substantially soil temperature estimations (Figure S4), and as such it enhanced confidence across the wintertime period. We found that SPA supports the main finding from our previous analysis on flux responses to meteorological variations and biological disturbance using observational data only (López-Blanco et al., 2017). In this study, large meteorological variability across the full annual 2008–2015 period led to a strong coupling between modelled photosynthetic inputs and respiration outputs and thus also stability of net C uptake (Figure 4). Wintertime plays an important role in the annual C budget by decreasing the C sink strength, mainly through sustained R_{eco} rates driven by C litter decomposition. We also note evidence that heterotrophic respiration dominates the shoulders of the growing seasons (wintertime, early spring, and late autumn), while growth and maintenance respiration are more important between greenup and greendown (Figure 5). From our sensitivity analysis of vegetation-related input parameters, it emerges that plant traits are important controllers in the interannual gross flux variability (Table 1). Also, we found that the sensitivity of both GPP and R_{eco} to changes in plant traits was coupled across meteorological variation (Figure 6).

3.1. Sensitivity and Quality of Modelled C Fluxes and Stocks

In this study, % of greenness data were used to constrain LAI simulated in SPA, defining the timing of the plant phenology at the beginning and at the end of the growing season (Figure 2a and Table 2). The % of

Table 2 *(continued)*

		Calibration set				Total
	Statistics	2013	2014	2015	2012–2015	2008–2015
NEE	Intercept	−0.1 (−0.14/−0.07)	0.02 (−0.05/0.1)	−0.1 (−0.15/−0.05)	−0.09 (−0.11/−0.06)	−0.13 (−0.15/−0.11)
	Slope	0.55 (0.51/0.59)	0.67 (0.59/0.75)	0.62 (0.56/0.68)	0.56 (0.54/0.59)	0.6 (0.57/0.62)
	R^2	0.85	0.82	0.8	0.81	0.73
	RMSE	0.21	0.25	0.25	0.24	0.29
	Bias	−0.02	0.19	−0.01	0.02	−0.07
GPP	Intercept	0.28 (0.2/0.36)	0.6 (0.35/0.85)	0.25 (0.12/0.38)	0.17 (0.11/0.24)	0.08 (0.02/0.13)
	Slope	0.8 (0.75/0.84)	1.1 (0.95/1.2)	0.75 (0.69/0.81)	0.69 (0.66/0.72)	0.76 (0.73/0.79)
	R^2	0.91	0.84	0.83	0.81	0.73
	RMSE	0.31	0.41	0.4	0.45	0.55
	Bias	0.59	0.47	0.67	0.73	0.42
Reco	Intercept	−0.28 (−0.33/−0.24)	−1.1 (−1.22/−0.95)	−0.23 (−0.27/−0.18)	−0.2 (−0.23/−0.16)	−0.16 (−0.18/−0.14)
	Slope	0.73 (0.68/0.77)	1.4 (1.3/1.6)	0.6 (0.56/0.64)	0.53 (0.5/0.56)	0.59 (0.56/0.61)
	R^2	0.73	0.56	0.7	0.52	0.5
	RMSE	0.24	0.34	0.24	0.34	0.36
	Bias	−0.51	−0.66	−0.57	−0.67	−0.52
LAI	Intercept	0.31 (0.31/0.31)	0.31 (0.31/0.32)	0.31 (0.31/0.32)	0.31 (0.31/0.31)	0.31 (0.31/0.31)
	Slope	0.07 (0.07/0.08)	0.07 (0.07/0.08)	0.07 (0.07/0.08)	0.07 (0.07/0.08)	0.07 (0.06/0.07)
	R^2	0.87	0.88	0.90	0.88	0.85
	RMSE	0.01	0.01	0.00	0.01	0.01
	Bias	0.12	0.08	0.12	0.10	0.08

greenness is only shown within the snow-free period, defined by the gray boxes across the entire time series. The modelled LAI was able to represent ~85% of the % of greenness variability (Table 2). The calibration set (2012–2015) has larger degree of agreement (R^2 = 0.88) compared to the validation set (2010–2011; R^2 = 0.83). NPP allocated to foliage, photosynthetic parameters, turnover rate of foliage, and maximum foliar carbon stock were key parameters used to fit the observations (Table 1). The modelled C stocks obtained from the labile, foliage, stem, root, and litter stocks and the observational data points from the field campaign in 2015 are included as mean ± range (Figure 2b). The field data on C stocks was used to establish a benchmark for each C stock at the modelled time step, assuming steady state conditions. The manual calibration aimed to have the modelled C stock inside the observations' ranges. Estimated C foliage, C stem, C roots, and C litter were within the observed thresholds (Figures 2b and S5). NPP allocated to foliage and roots (Figure 2c), as well as all the turnover rate parameters (Figure 2d) and the initial C stocks were key to estimating ecosystem C stocks.

The SPA estimates of C fluxes across eight snow-free periods were validated against the flux data presented in López-Blanco et al. (2017; Figure 3). The model represented ~73%, ~73%, and 50% of the variability in NEE, GPP, and R_{eco}, respectively (Table 2). The calibration set has a larger degree of agreement (R^2 = 0.81, 0.81 and RMSE = 0.24, 0.45 for NEE and GPP, respectively) compared to the validation set (R^2 = 0.70, 0.77 and RMSE = 0.24, 0.45), except for R_{eco} (R^2 = 0.52 in calibration versus R^2 = 0.59 in validation; Table 2). The mean annual NEE during the 2008–2015 period was −17.2 g C m^{-2} (range −33.8 to 5.3 g C m^{-2}), while mean GPP was −147.9 g C m^{-2} (−92.8 to −219.4 g C m^{-2}) and mean R_{eco} was 130.7 g C m^{-2} (98.1 to 185.6 g C m^{-2}; Table 3). In general, the model captured the initial respiration peak of the growing season (Figure 3a) and the beginning of the growing season (R^2 = 0.85, $p < 0.001$), followed by a short but intensive C uptake period (Figures 3a and 3c). However, Figures 3b and 3d also show the biases observed due to difference in timing (shifts of peak of the growing season in 2010 R_{eco} and 2011 NEE for example) and differences in flux magnitudes (such as 2012 GPP and R_{eco}). Overall, SPA tended to overestimate NEE (i.e., higher C uptake) by 13%, while GPP and R_{eco} were underestimated (i.e., lower photosynthetic and respiration rates) by 28% and 36%, respectively.

LMA, rate coefficient for J_{max} (J_{max}), maximum foliar mass, and foliar nitrogen (N) are the four most sensitive parameters in SPA for the simulation NEE, GPP, and R_{eco} under the current setup (Table 1). For example, the S-

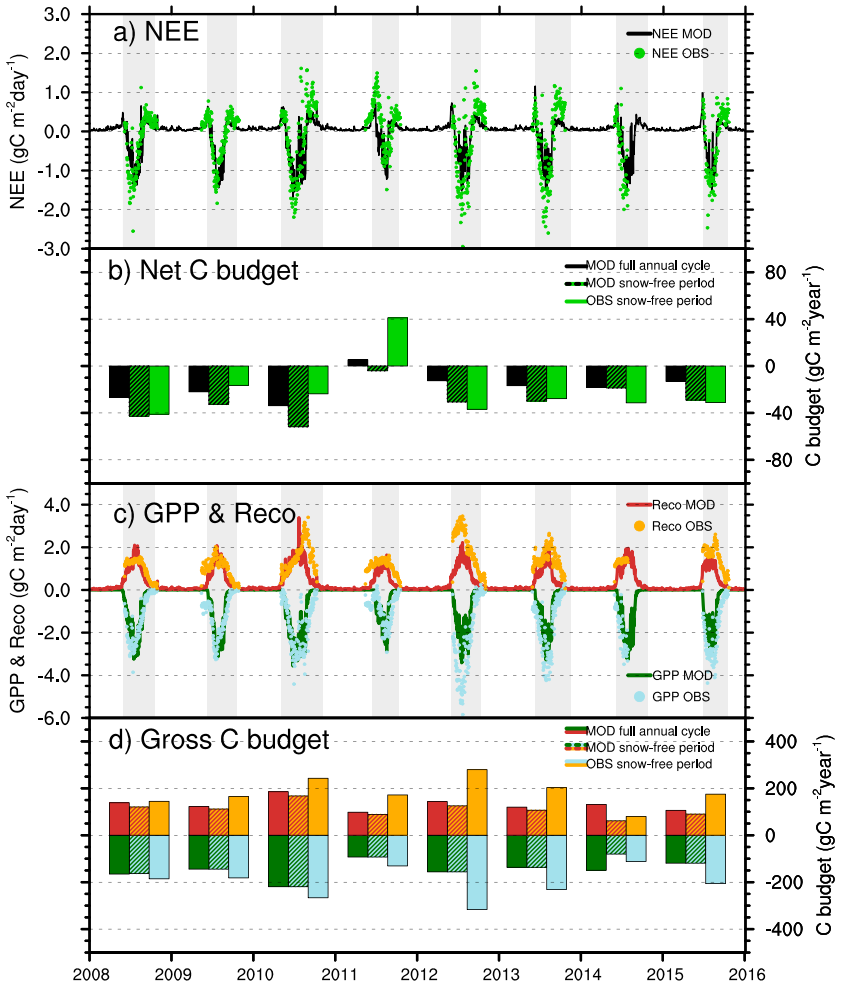

Figure 3. Time series (a and c) and full annual budgets (b and d) of observed (OBS) and predicted (MOD) C fluxes (NEE, net ecosystem exchange; GPP, gross primary production; and R_{eco}, ecosystem respiration).

index of LMA (SI-NEE = 4.55) denotes that if this parameter increases 1%, C fluxes will experience a shift of 4.55%. Interestingly, NEE, GPP, and R_{eco} experienced a similar sensitivity pattern, and SI-GPP and SI-R_{eco} were in the same order of magnitude. LMA, maximum foliar mass, and foliar N are field observations collected in the 2015 field campaign; thus, this sensitivity analysis demonstrates how field data can help to improve the model certainty over key parameters. However, there are other calibrated parameters such as mineralization rate of SOM or fraction of leaf loss to litter that are relatively sensitive for the modelled C fluxes, denoting site-specific characteristics with likely high uncertainty if they are applied to different conditions/locations. Ideally, the calibrated parameters need to be replaced by field measurements from similar conditions to improve the certainty around the SPA runs in case model is to be applied to other sites.

3.2. The Role of the Winter Period on the Full Annual-Cycle C Balance

The SPA model quantifies the wintertime period in the annual C budget. The addition of the respiratory losses across wintertime periods shifted NEE significantly by decreasing the C sink strength ~60% (Figures 3b, 3d, and 4) and increasing 22.7% the annual soil respiration ($R_{g\ root} + R_{m\ root} + R_{h\ litter} + R_{h\ soil\ organic\ matter}$) excluding the June–September period. Interestingly, the partitioning of these wintertime respiration losses indicates that $R_{h\ litter}$ was the largest contributor with 43.3% to the annual budget. During winter, the only two flux contributions to NEE were derived from litter and SOM decomposition, both parts of the heterotrophic

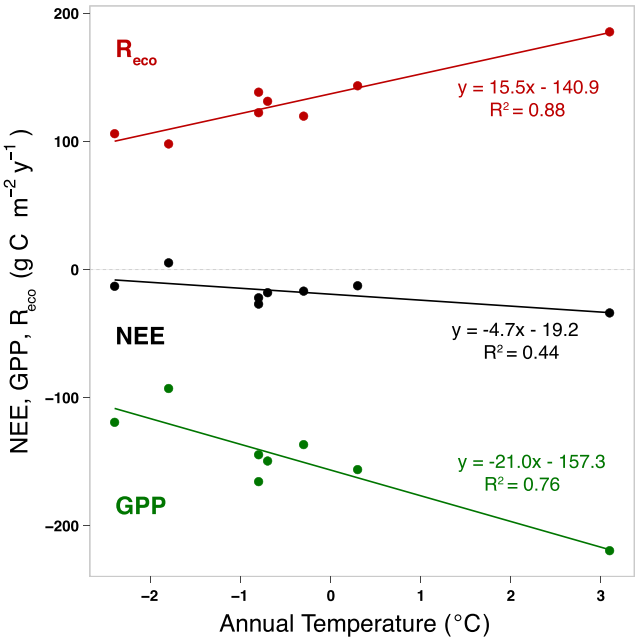

Figure 4. The relationship between estimated annual NEE (black), GPP (dark green), R_{eco} (dark red) (g C m^{-2} $year^{-1}$) and mean annual temperature (°C) for the years 2008–2015. Linear regressions are shown for each flux against temperature, including equations and R^2 values.

respiration (R_h; Figure 5a; Equation S1). The contribution from litter decomposition to the annual budget is 2-fold larger than from SOM (27% versus 15%). Moreover, in Arctic ecosystems there are two key periods with large respiratory losses (i.e., large positive NEE) in the transition between summer and the shoulder seasons (Figure 3a). The first peak is between the end of the snow melt period and the beginning of growing season, while the second one is observed between the end of the growing season and the freeze-in period. The model suggests that the first peak of positive NEE was driven by air temperature ($R^2 = 0.77$, $p < 0.001$), while the second peak was driven by the accumulation of litter stock ($R^2 = 0.74$, $p < 0.001$). These two processes occurred in spring and fall together with the respiration produced by litter and SOM in winter are the main contributors to the decrease of C sink strength.

Since the validation of wintertime fluxes remains challenging due to the lack of field data, we constrained the snow cover, one of the most important controllers of the wintertime period in Arctic ecosystems, and its direct influence on soil temperature and therefore the C fluxes. The agreement between observed and modelled soil temperatures at 10 cm depth was ~94% with snow cover routine employed and ~65% without (Figure S4). The major improvement on the model simulations was for wintertime soil temperatures, which on average increased from −9.1 to −0.6 °C (observations were −0.3 °C) for the January–April period and from −0.6 °C to +2.4 °C (observations were +2.8 °C) for the November–December period. Moreover, these changes in soil temperature (i.e., warmer temperatures in wintertime) have increased R_h (litter + SOM) ~8% due to the insulation effect from snow.

3.3. Partitioning the Processes Contributing to NEE and Their Meteorological Sensitivity

We found that SPA supports the main finding from our previous analysis on flux responses to meteorological variations and biological disturbance (López-Blanco et al., 2017). The net C uptake insensitivity found across meteorologically diverse growing seasons and full annual cycles here is also driven by the compensation between photosynthesis (GPP) and the sum of respiration losses (R_{eco}; Figures 4 and 5). The model suggests stronger and steeper correlations between annual GPP ($R^2 = 0.75$, slope = 21 g C m^{-2} $year^{-1}$ °C) and R_{eco} ($R^2 = 0.88$, slope = 15 g C m^{-2} $year^{-1}$ °C) with annual temperatures compared to NEE-temperature ($R^2 = 0.44$ and slope = 5 g C m^{-2} $year^{-1}$ °C; Figure 4). These results reinforce previous findings demonstrating a relative insensitivity of NEE to meteorological drivers, due to the compensatory effect between GPP and R_{eco} shown here. A linear regression of annual R_{eco} on GPP shows a strong correlation, $R^2 = 0.96$. We note evidence that R_h dominates the outer shoulders (wintertime, early spring, and late autumn), while R_g and R_m are more important during the growing season (Figure 5a). In summer, plant growth increased R_a. Annually aggregated data suggest that when R_a was dominating over R_h, there was a tight link between GPP and R_{eco}. The annual data also reflect a strong relationship between GPP and R_a ($R_m + R_g$) ($R^2 = 0.97$, $p < 0.001$). Phenology drivers such as beginning of the growing season ($R^2 = 0.88$ and 0.82, $p < 0.001$) and snow melt period ($R^2 = 0.82$ and 0.89, $p < 0.001$) played an important role in the GPP and R_a dynamics, respectively (Figure S6). We also found a significant correlation between GPP and R_h ($R^2 = 0.89$, $p < 0.001$), influenced by the amount of litter deposited each year (proportional to GPP), as noted from the major contribution from litter decomposition to R_h. Overall, annual photosynthetic inputs dominate the sum of the respiration outputs ($R_g + R_m + R_h$) except in 2011 (Figure 5b).

Interestingly, the model quantified a decrease of 20% in the annual CUE for 2011. This decrease was directly related to a significant decrease of GPP (40%) and R_a (34%) compared to the rest of the years (Table 3). Moreover, annual R_h increased its contribution to NEE ~18% in 2011, likely induced by the late snow melt period. These estimations are the result of a marked variability of meteorological conditions between 2010 and 2011. Even though the Kobbefjord area was associated with a major larvae outbreak (Lund et al., 2017), the

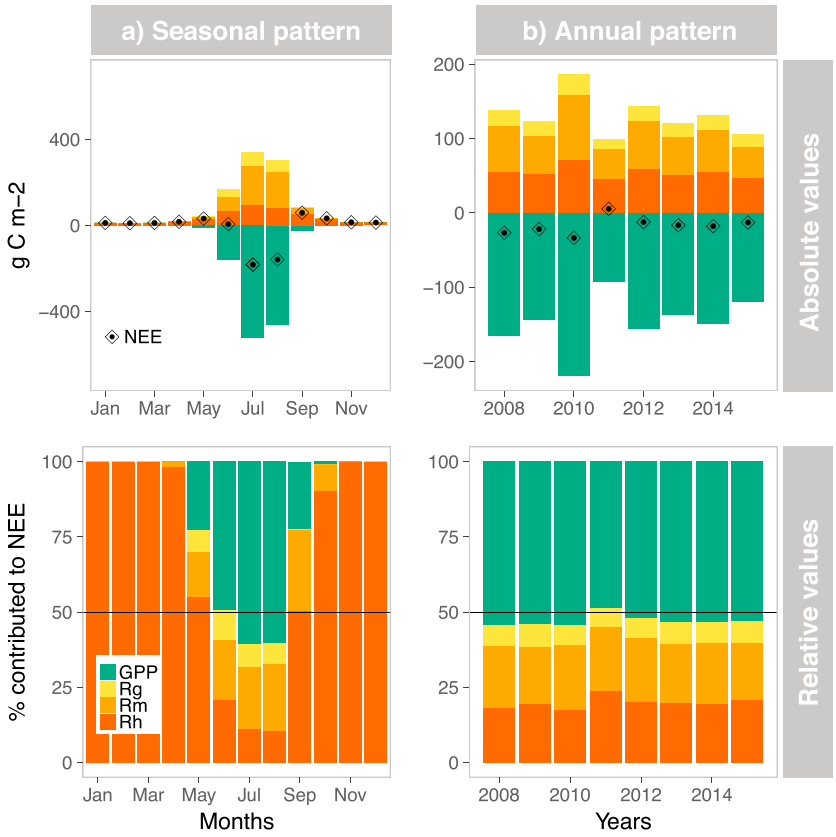

Figure 5. Seasonal (a) and annual (b) partitioned modelled gross fluxes (GPP, gross primary production; R_g, growth respiration; R_m, maintenance respiration; and R_h, heterotrophic respiration). The upper set shows absolute values including superimposed monthly and annual NEEs. The bottom set shows relative values (i.e., the % contributed of gross fluxes to NEE) highlighting the balance between inputs (productivity) and outputs (respiration).

model unexpectedly captured the seasonality of NEE without any prescription in the model structure on biological disturbances. The model was able to estimate similar NEE ($R^2 = 0.76$, $p < 0.001$), GPP ($R^2 = 0.80$, $p < 0.001$) and R_{eco} ($R^2 = 0.65$, $p < 0.001$) in 2011 when we run the C uptake seasonality in SPA forced by the % of greenness data instead (compared to the regular set up; $R^2 = 0.42$, 0.51 and 0.66, $p < 0.001$ respectively; Table 2). The NEE estimates from this synthetic setup (18 g C m^{-2}) were still not close to the field measurements (40 g C m^{-2}), but they were better than environmental driven runs (5 g C m^{-2}). Therefore, SPA quantifies the likely effect on 2011 NEE as 45% meteorological driven and 55% contributed by the moth outbreak in 2011 from the difference between the phenology driven run and the field observations. This finding suggests a joint, relatively equal influence from both the meteorological drivers and the biological disturbance.

3.4. The Plant Traits Effect on Buffering the Interannual NEE Variability

We found that both GPP and R_{eco} are sensitive to annual temperature variability, while NEE is much less sensitive due to compensatory effects (Figure 4). In order to understand the reason of this compensation, we hypothesized that plant traits couple the two processes closely and lead to compensation. Plant traits such as LMA, rate coefficient for J_{max}, maximum leaf mass, and foliar N are the most sensitive controls on both GPP and R_{eco} shown by the sensitivity analysis (Table 1), which provides some support for our hypothesis. For further testing, we repeated the sensitivity experiments for individual years (2008–2015) and these four plant traits (Figure 6). We assessed the regression lines describing the change in GPP and R_{eco} trait sensitivity to mean annual temperature using two analysis of covariance tests with and without the interaction between GPP and R_{eco}. The models with interaction were not significantly different, which suggests the slopes of the relationships do not differ between GPP and R_{eco} fits. Thus, the emergent relative temperature sensitivity of

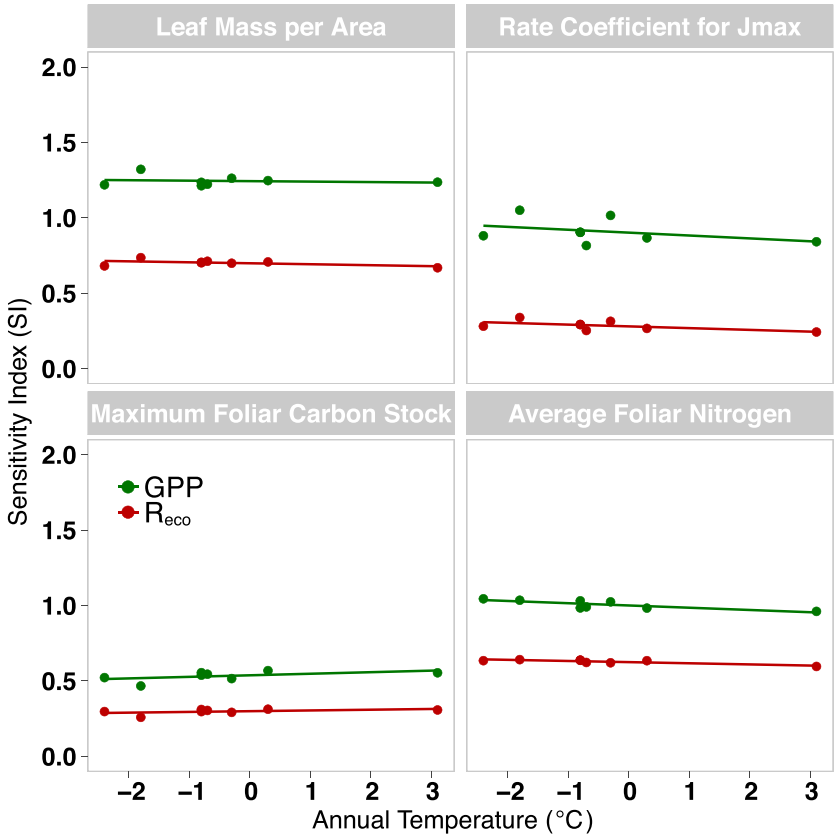

Figure 6. Sensitivity variability of the four most sensitive parameters in soil-plant-atmosphere (shown in Table 1) compared to the mean annual temperature through the analyzed years (2008–2015).

these processes, and therefore compensation, is maintained despite potential year to year or spatial differences in plant traits.

4. Discussion

The SPA model has been implemented, calibrated, and validated to explore the challenges in process based understanding of C cycling in Arctic ecosystems at high temporal resolution (i.e., half-hourly time

Table 3
Annual Average of Main Ecosystem C Fluxes NEE, GPP, NPP and R_{eco}

Years	NEE	GPP	NPP	R_{eco}	$R_{m\ leaf}$	$R_{m\ root}$	$R_{g\ leaf}$	$R_{g\ root}$	$R_{g\ stem}$	$R_{h\ litter}$	$R_{h\ som}$	CUE
2008	−26.9	−165.5	−80.8	138.5	43.4	19.2	7.8	9.2	4	36.1	18.8	0.49
2009	−22	−144.5	−70.4	122.5	34.7	16.4	7.8	8.2	3.5	34.2	17.6	0.49
2010	−33.8	−219.4	−104.8	185.6	59.9	27.2	7.8	13.6	5.8	43.7	27.5	0.48
2011	5.3	−92.8	−35.2	98.1	25	15.3	7.8	3.1	1.3	29.6	16	0.38
2012	−12.6	−156.1	−71.5	143.5	43.1	20.5	7.9	8.4	3.6	38.1	21.9	0.46
2013	−16.8	−136.6	−64.3	119.8	35.1	15.7	7.8	7.3	3.1	33.1	17.5	0.47
2014	−18	−149.4	−70	131.4	39.5	17.7	7.8	8.1	3.5	35.2	19.5	0.47
2015	−13	−119.2	−56.9	106.1	28.2	14.3	7.8	6.3	2.7	31	15.9	0.48
Mean 2008–2015	−17.2	−147.9	−69.2	130.7	38.6	18.3	7.8	8.0	3.4	35.1	19.3	0.47
Min 2008–2015	−33.8	−219.4	−104.8	98.1	25.0	14.3	7.8	3.1	1.3	29.6	15.9	0.38
Max 2008–2015	5.3	−92.8	−35.2	185.6	59.9	27.2	7.9	13.6	5.8	43.7	27.5	0.49

Note. NPP is defined as NPP = GPP − R_a. R_{eco} sub-subcomponents split between the autotrophic respiration (R_a; the sum of growth (R_g) and maintenance (R_m) respiration from leaves, stems and roots) and heterotrophic respiration (R_h; litter and soil organic matter decomposition). Carbon use efficiency (CUE) is defined as CUE = 1 − ((R_m + R_g)/GPP). The units for all variables are g C m^{-2} $year^{-1}$ except for CUE (dimensionless).

steps). The model captured well multiseason and multiannual variability of plant phenology and C dynamics compared to field observations. The results here are in line with a previous study showing meteorology driven insensitivity of NEE based on the coupling between GPP and R_{eco}, also throughout full annual cycles. However, the results from this paper also point to plant traits as key controls in the compensatory effect between GPP and ecosystem respiration. This study emphasizes the significance of integration between field observations and process-based modeling to advance our understating of ecosystem carbon dynamics.

4.1. Quality and Limitations of Modelled C Fluxes and Stocks

The SPA model demonstrated a coherent performance of basic C fluxes, stocks and plant phenology against the independent in situ data provided by the GEM program (Figures 2a and 2b, Figure 3, and Table 2). In this modeling exercise, three important sources of data are vital for model performance: (1) plant phenology (i.e., the % of greenness; Figure 2a and Table 2); (2) the snow fraction information (Figure S3), both derived from an inexpensive optical camera (Westergaard-Nielsen et al., 2013; Westergaard-Nielsen et al., 2017); and (3) the foliar N content and LMA data from the field campaign (Figure S2 and Table 1). On the one hand, the fit between observed and modeled beginning of the growing season ($R^2 = 0.92$; $p < 0.001$) was a major challenge, and it has been found very sensitive for the simulated C budget. Mismatches on growing season start/end led to significant biases, both positive and negative (Table 2), likely shaped by the high meteorological interannual variability observed in Kobbefjord (López-Blanco et al., 2017). For example, the model underrepresented phenology dynamics between years 2010 and 2011, with a subsequent impact on C budget estimations. In 2010, the warmest summer with the longest growing season triggered an excessive C uptake, while in 2011 the colder June followed by the cloudier July likely led to a delayed growing season, not well captured in SPA. By forcing SPA's beginning of the growing season in 2011 with the % of greenness data (rather than environmentally forced), the agreement improved from a $R^2 = 0.4$ to $R^2 = 0.76$ for NEE, and an increase of 18 g C m^{-2} respired. Along these lines, this is also an indirect validation of the phenology methodology and its links to C dynamics.

On the other hand, three of the most sensitive parameters used in the model runs (LMA, J_{max}, and maximum foliar mass) were derived from field observations (Table 1). The terrestrial carbon cycle is currently the least constrained component of the global carbon budget (Bloom et al., 2016; IPCC, 2013). From a modeling perspective, more field measurements are required to better constrain the ecosystem model performances of C cycling in changing environments. We consider that more observations on plant phenology, photosynthetic parameters (Albert et al., 2011; Boesgaard et al., 2012; Rogers et al., 2017), plant structure (Campioli et al., 2013; Van Wijk et al., 2004), C and N stocks at different stages of the season (Arndal et al., 2009), C storage and turnover (Cornelissen et al., 2007; DeMarco et al., 2014; Hobbie et al., 2000; Sloan et al., 2013) will improve modeling robustness based on enhanced calibrations. The discussion around variable selection, experimental design, and data suitability needs to be agreed both by field and model researchers. The incorporation of field observations into models can lead to improvements in modelled ecosystem processes, while models can inform on data collected in field campaigns.

The SPA model outputs, which has been manually parameterized (Table 1), could benefit from model data fusion approaches based on Bayesian statistics and optimal parameter sets (Bloom et al., 2016; Bloom & Williams, 2015; Williams et al., 2005). Additionally, we have neglected important components and processes shaping more complete C dynamics in northern latitudes. First, mosses should be considered in Arctic tundra modeling studies (Uchida et al., 2016) as they are a representative vegetation type in Arctic ecosystems and have important implications for CUE and soil temperature insulation (Bradford & Crowther, 2013; Street, Stoy, et al., 2012; Street et al., 2013; Williams et al., 2000). Second, methane (CH_4) is another important contributor to the total C budgets in these ecosystems (Mastepanov et al., 2008, 2012; Tagesson et al., 2012; Zona et al., 2016). However, CH_4 modeling is challenging due to its different transport mechanisms, but possible (Kaiser et al., 2017; Walter et al., 2001; Walter & Heimann, 2000), and some studies can be used to set up future modeling efforts at this site (Pirk et al., 2017). Third, permafrost dynamics brings an additional layer of complexity to the C exchange (Åkerman & Johansson, 2008; Koven et al., 2011; Schuur et al., 2015) and its application and modeling is required due to the increased permafrost thaw in warmer temperatures (Rasmussen et al., 2017; Riseborough et al., 2008). Fourth, dissolved organic carbon losses by runoff can represent 12–35% of NEE in similar latitudes (Olefeldt et al., 2012; Roulet et al., 2007), and fen sites have been found to have higher export

rates than bogs or palsa environments (Olefeldt & Roulet, 2012). Finally, vegetation shifts feedbacks in response to changing temperature, precipitation, snow dynamics, and permafrost thaw are critical (Andrew et al., 2017; Myers-Smith et al., 2015), and its modeling has been proved implementable (van der Kolk et al., 2016).

4.2. The Role of the Winter Period on the Full Annual-Cycle C Balance

Recent studies have emphasized the relevance of the incorporation of wintertime periods to gain a more comprehensive understanding of the C sink/source dynamics in Arctic terrestrial ecosystems (Commane et al., 2017; Zona et al., 2016). The response of decomposition processes to temperature across long and cold winters is critical, especially when low but constant rates of respiration contribute to the annual budget under changing snow packs (McGuire et al., 2000). Thick snow packs insulate the soil from low temperatures and can at the same time act as a lid preventing respiration losses from reaching the atmosphere until snowmelt period (Lund et al., 2012). In this study, we included snow fraction data (Figure S3) to constrain soil temperature (Figure S4), so the representation of heterotrophic respiration derived from roots, litter and SOM decomposition in the outer shoulders (Figure 3) is more realistically simulated. Hobbie et al. (2000) indicated that winter activity can influence both the magnitude and the direction of annual C fluxes, and they reported winter activity to represent 61–81% of annual NEE (Oechel et al., 1997) and ~20% of annual soil respiration (Schimel & Clein, 1995). Here we quantify a decrease of the C sink strength (NEE) of 62% and an increase of 22.7% of the annual soil respiration. This result suggests a nontrivial contribution of the cold period to the year-round CO_2 exchange in this tundra site. The challenges now remain on wintertime-based field campaigns, similar to Pirk et al. (2016), to measure soil CO_2 data for validation with certain temporal coverage. To better constrain the decomposition rates and their feedbacks with snow regimes and soil temperatures controlling the wintertime C dynamics in Arctic ecosystems, it is essential to increase efforts on monitoring the changes occurring over full annual cycles (Euskirchen et al., 2012; Grøndahl et al., 2008), and at a deeper level of complexity (Cornelissen et al., 2007; DeMarco et al., 2014).

4.3. Quantifying the Contributing Processes to NEE, Their Meteorological and Biological Sensitivity, and Links to Leaf Traits

The SPA model has proven capable of effectively simulating Arctic C cycling (Table 2) at a very high temporal resolution as a result of its parameterization at leaf-level scale (Table 1), unravelling deeper levels of complexity at canopy-level scale (Table 3). In SPA, the net C uptake was calculated from the balance between the photosynthetic inputs (GPP) and respiration outputs (R_{eco}; Figure 3), and the respiration losses are separated into its finer components (R_g, R_m, and R_h) (Figure 5). In the biosphere, stock dynamics are connected (Dopheide et al., 2012), and these fluxes are the result of the allocation (Figure 2c) of NPP to the various identifiable stocks of biomass (foliage, labile, stems, roots, litter, and SOM) together with their turnover rates and decomposition (Figure 2d). SPA captures all these fluxes within the same framework, and Figure 7 is an illustration of the terrestrial C cycling in Kobbefjord the period 2008–2015. Figure 7 synthesizes annual ranges of C stocks, allocation, turnover, and fluxes shown previously in Figures 2, 3, 4, and 5b and Table 3. The sensible balance between the components (Figure 7) can be highly dependent on meteorological variability but also biological disturbances (López-Blanco et al., 2017). In fact, one can positively feedback on the other. For example, in 2010, Kobbefjord experienced the warmest July–September period, and this anomaly was followed by a colder and drier October-May period, producing the thickest snowpack (Figure S1) on record. Additionally, the delayed beginning of the growing season in 2011 was characterized by a colder June, a cloudier (low PAR) July (Table S1) and larvae moth feeding on vegetation surrounding the fen (Lund et al., 2017). This succession of meteorological and biological events may have favored (1) optimal conditions for the moth outbreak, facilitating the survival of larvae eggs over winter due to the warmer soil temperatures under a very thick snowpack and (2) minimal conditions for plant growth agreeing with the significant decrease in GPP (Figure 5b) and subsequent decrease of CUE (Table 3). This study demonstrates that shifts in growing season timing can lead to large changes in net C exchange, thus delayed effects can severely affect the following years' performance.

However, SPA representation of process interactions agrees with the analyses realized by López-Blanco et al. (2017), suggesting that large interannual growing season variability of GPP and R_{eco} are also compensatory, and so NEE remained stable across meteorologically diverse years (Figure 4 and 5b). This result can be compared with the findings from Westergaard-Nielsen et al. (2017) in Zackenberg, Northeast Greenland, where

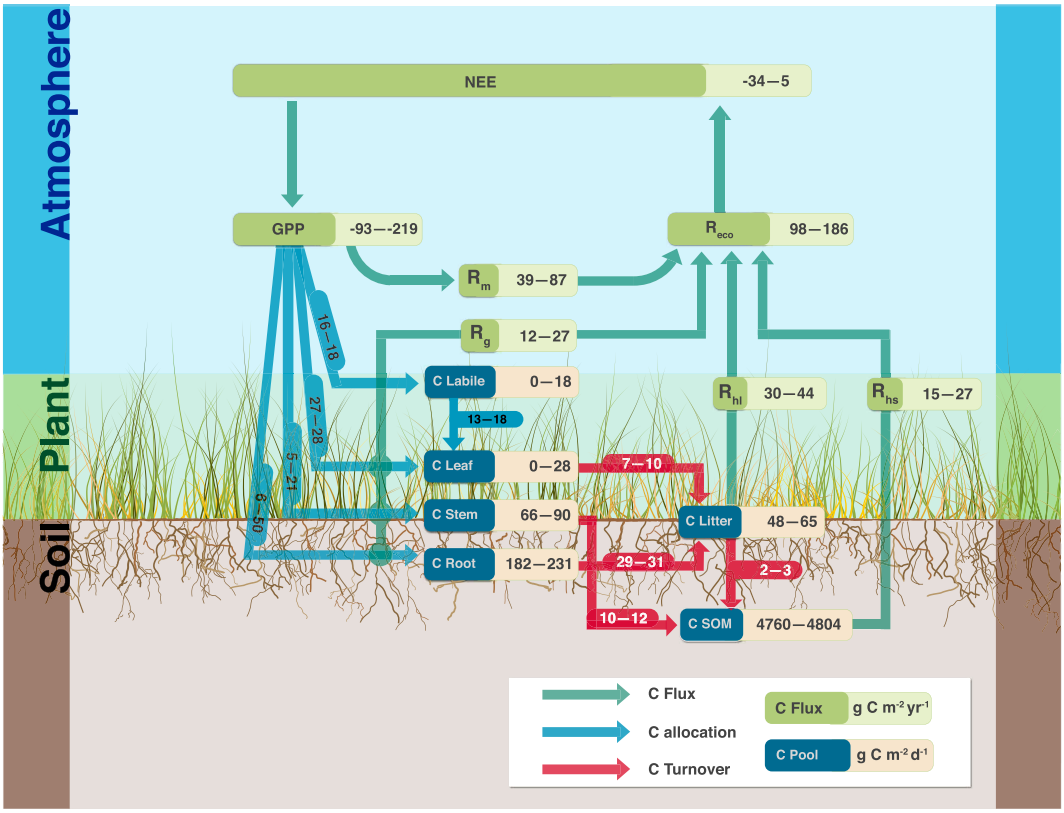

Figure 7. Schematic diagram of the terrestrial C processes modelled in SPA for the Kobbefjord (fen) site across the soil-plant-atmosphere continuum. C processes represented include flows for C fluxes in green (NEE, net ecosystem exchange; GPP, gross primary production; R_{eco}, ecosystem respiration; R_g, growth respiration; R_m, maintenance respiration; and R_h, heterotrophic respiration), C allocation in light blue (to labile, leaf, stem, and root), C turnover in dark red (from leaf, stem, root, and litter) and C stocks in dark blue (labile, leaf, stem, root, litter, and SOM). The ranges delimit minimum and maximum values.

the vegetation compensated the shorter growing season by having fast greenup and a tendency to higher peak in greenness, which links to GPP. We use the modeling to explore the mechanisms driving this compensatory effect. We implemented tissue-level respiration-nitrogen relationships from Reich et al. (2008) and fixed fractions of C allocated following Waring and Schlesinger (1985) to dynamically calculate R_m and R_g, respectively (Figure 5). During the June–August period, R_a contributed 69.8% to all respiratory losses (R_{eco}; R_g = 18.5%; R_m = 51.25%; Figure 5a) while annually, 58.3% (R_g = 14.8%; R_m = 43.5%; Figure 5 b). These results suggest that the plant respiration is dominated by nitrogen-related dynamics (R_m) rather than the production of new biomass (R_g). The parameterization used here has been already reported based on plant C stock size and on the magnitude of GPP (Hopkins et al., 2013; Thornton & Rosenbloom, 2005). However, reports of explicit partitioned respiration components in the Arctic are missing, so field measurements are required for validation. Overall, this implementation provided a better understanding of the CUE responses to environmental change, and CUE estimations are more abundant in literature. The CUE around the sub-Arctic tundra has been reported ~0.47, but mosses could increase it up to 0.71–0.81 (Bradford & Crowther, 2013; Street et al., 2013). Here we reported CUE, estimated from first principles of modeling GPP and R_a, of ~0.5 except in 2011 (Table 3). We found CUE to be sensitive to the events described this year, decreasing from ~0.5 to 0.4 (Table 3). A value of 0.4 indicates that 40% of gained C is allocated to biomass, and thus the GPP-R_{eco} compensation was disrupted by an unusual meteorology and the biological disturbance. CUE is sensitive to temperature and nitrogen concentration (cold temperatures and large N availabilities will increase CUE; Bradford & Crowther, 2013). In likely warming scenarios the CUE is hypothesized to decrease, favoring respiration losses (Street et al., 2013); therefore, this fact may affect the future coupling. Further modeling studies can investigate this likelihood.

From the sensitivity analysis (Table 1), similar responses of NEE, GPP, and R_{eco} have emerged to changes in plant traits and vegetation properties. In fact, the correlation of GPP and R_{eco} sensitivity to the same key parameters was strong (R^2 = 0.84), supporting the compensatory effect revealed by GPP and R_{eco} (R^2 = 0.95; Table 3). Reichstein et al. (2014) suggested that a significant part of the large unexplained variance of ecosystem functional properties and their environment is related to variation in plant traits. Additionally, the same authors suggested that ecosystem properties such as GPP or R_a could be derived from plant traits, claiming also a stronger integration of plant traits and ecosystem-atmosphere exchange. Here LMA, the rate coefficient for J_{max}, maximum foliar mass, and foliar N were found to be very important elements for the model parameterization (Table 1). We also found that these four most sensitive N-related plant traits in SPA presented a similar temperature sensitivity for GPP and R_{eco} across full annual cycles (Figure 6). This evidence supports our hypothesis that plant traits drive stabilization of NEE (Figure 4), through temperature-sensitive compensation between GPP and R_a. We find that GPP is more sensitive to temperature than R_{eco}, so compensation is not completely balanced between GPP and R_{eco}. But both fluxes have similar trait-temperature sensitivity, and so compensation is relatively insensitive to temperature changes. There is evidence that plant traits are potentially key controllers in the gross flux coupling and that they can explain other ecosystem functional properties, including allocation, respiration and decomposition and stabilization of carbon in the soil. Street, Shaver, et al. (2012) pointed to very robust relationships between total foliar nitrogen and LAI across multiple different Arctic regions, despite their large variability in C uptake and plant functional types. The role of functional properties seems very important to interannual variability, even to biological disturbance, which suggests ecosystem resilience to changes (Reichstein et al., 2014). Further testing of the hypothesis presented here could involve a comparison of flux measurements from other high-latitude sites with similar climate but differing dominant vegetation communities, with different plant traits.

5. Conclusions

The SPA model captures well high temporal C dynamics and plant phenology in high-latitude ecosystems. Using a process model, we have explored the role of the wintertime period on NEE and decomposed the compensatory effects buffering NEE to meteorological variability. Wintertime heterotrophic respiration decreased the annual C sink strength mostly through litter decomposition, highlighting the importance of the cold period to the year-round CO_2 exchange in Arctic tundra. The modeling suggests that GPP and R_{eco} sensitivities to meteorology are similar and therefore compensatory, due to the key role that plant N content has on both processes, leading to a NEE stability across climatically diverse full annual cycles. Here plant traits and vegetation properties seem to be relevant controllers of the gross flux coupling. Continued exploration of flux time series is required to investigate the robustness of this meteorological buffering. Special attention needs to be paid to disturbance events such as the 2011 anomaly where the interplay between unusual meteorology and moth outbreak can break down the photosynthesis-respiration compensation.

Acknowledgments
The authors wish to thank the Nuuk Ecological Research Operations (nuuk-basic.dk) as well as the ClimateBasis programme, in charge of the meteorological stations, the GeoBasis programme, in charge of the eddy covariance system, and the BioBasis programme, especially to Maia Olsen, for the collection and shipping of vegetation and soil samples. Both projects are being run under the GEM program funded by the Danish Environmental Protection Agency and the Danish Energy Agency. Moreover, this work was supported in part by a scholarship from the Aarhus-Edinburgh Excellence in European Doctoral Education Project and by the eSTICC (eScience tools for investigating Climate Change in Northern High Latitudes) project, part of the Nordic Center of Excellence (57001), as well as the Danish National Research foundation (DNRF100). We acknowledge the support of the NERC CYCLOPS and GREENHOUSE projects. Thanks are also due to Isabel de Andrés Velasco for contribution on the artistic design in Figure 7. Measurement data from the GEM program are freely available from the GEM database (http://data.g-e-m.dk/). The SPA model version used in this study (cyclops version—2.6.0.cyclops) is freely available from the SPA's developer page (https://sourced.ecdf.ed.ac.uk/projects/geos/SPA). Instructions on how to get the source code and how to compile and run SPA are available from the SPA Users Wiki (https://www.wiki.ed.ac.uk/display/SPA/SPA+Model). Postprocessed data and scripts are available from the authors upon request (elb@bios.au.dk).

References

ACIA (2005). *Arctic climate impact assessment*. New York: Cambridge University Press.

Åkerman, H. J., & Johansson, M. (2008). Thawing permafrost and thicker active layers in sub-arctic Sweden. *Permafrost and Periglacial Processes*, *19*(3), 279–292. https://doi.org/10.1002/ppp.626

Albert, K. R., Ro-Poulsen, H., Mikkelsen, T. N., Michelsen, A., Van Der Linden, L., & Beier, C. (2011). Effects of elevated CO2, warming and drought episodes on plant carbon uptake in a temperate heath ecosystem are controlled by soil water status. *Plant, Cell & Environment*, *34*(7), 1207–1222. https://doi.org/10.1111/j.1365-3040.2011.02320.x

AMAP (2017). Snow, water, ice and permafrost in the Arctic (SWIPA) 2017. Retrieved from Oslo, Norway: https://www.amap.no/documents/doc/Snow-Water-Ice-and-Permafrost-in-the-Arctic-SWIPA-2017/1610

Andrew, C. M., Elizabeth, S. J., Gillian, P., Isla, M.-S., & Marc, M.-F. (2017). Shrub growth and expansion in the Arctic tundra: an assessment of controlling factors using an evidence-based approach. *Environmental Research Letters*, *12*(8), 085007.

Arndal, M. F., Illeris, L., Michelsen, A., Albert, K., Tamstorf, M., & Hansen, B. U. (2009). Seasonal variation in gross ecosystem production, plant biomass, and carbon and nitrogen pools in five high Arctic vegetation types. *Arctic, Antarctic, and Alpine Research*, *41*(2), 164–173. https://doi.org/10.1657/1938-4246-41.2.164

Aurela, M., Laurila, T., & Tuovinen, J.-P. (2004). The timing of snow melt controls the annual CO_2 balance in a subarctic fen. *Geophysical Research Letters*, *31*, L16119. https://doi.org/10.1029/2004GL020315

Bay, C., Aastrup, P., & Nymand, J. (2008). The NERO line. A vegetation transect in Kobbefjord, West Greenland. Retrieved from

Bintanja, R., & Andry, O. (2017). Towards a rain-dominated Arctic. *Nature Climate Change*, *7*, 263. https://doi.org/10.1038/nclimate3240

Black, T. A., Chen, W. J., Barr, A. G., Arain, M. A., Chen, Z., Nesic, Z., et al. (2000). Increased carbon sequestration by a boreal deciduous forest in years with a warm spring. *Geophysical Research Letters*, *27*(9), 1271–1274. https://doi.org/10.1029/1999GL011234

Bloom, A. A., Exbrayat, J.-F., van der Velde, I. R., Feng, L., & Williams, M. (2016). The decadal state of the terrestrial carbon cycle: Global retrievals of terrestrial carbon allocation, pools, and residence times. *Proceedings of the National Academy of Sciences*, *113*(5), 1285–1290. https://doi.org/10.1073/pnas.1515160113

Bloom, A. A., & Williams, M. (2015). Constraining ecosystem carbon dynamics in a data-limited world: integrating ecological "common sense" in a model–data fusion framework. *Biogeosciences*, *12*(5), 1299–1315. https://doi.org/10.5194/bg-12-1299-2015

Boesgaard, K. S., Albert, K. R., Ro-Poulsen, H., Michelsen, A., Mikkelsen, T. N., & Schmidt, N. M. (2012). Long-term structural canopy changes sustain net photosynthesis per ground area in high arctic Vaccinium uliginosum exposed to changes in near-ambient UV-B levels. *Physiologia Plantarum*, *145*(4), 540–550. https://doi.org/10.1111/j.1399-3054.2011.01564.x

Bradford, M. A., & Crowther, T. W. (2013). Carbon use efficiency and storage in terrestrial ecosystems. *New Phytologist*, *199*(1), 7–9. https://doi.org/10.1111/nph.12334

Callaghan, T. V., Johansson, M., Brown, R. D., Groisman, P. Y., Labba, N., Radionov, V., et al. (2012). The changing face of arctic snow cover: A synthesis of observed and projected changes. *Ambio*, *40*(1), 17–31. https://doi.org/10.1007/s13280-011-0212-y

Campioli, M., Schmidt, N., Albert, K., Leblans, N., Ro-Poulsen, H., & Michelsen, A. (2013). Does warming affect growth rate and biomass production of shrubs in the High Arctic? *Plant Ecology*, *214*(8), 1049–1058. https://doi.org/10.1007/s11258-013-0230-x

Christensen, J. H., Hewitson, B., Busuioc, A., Chen, A., Gao, X., Held, I., et al. (2007). Regional climate projections. In S. Solomon, et al. (Eds.), *Climate Change 2007: Climate Change 2007: The Physical Science Basis: Working Group I Contribution to the Fourth Assessment Report of the IPCC* (pp. 848–940). New York: Cambridge University Press.

Commane, R., Lindaas, J., Benmergui, J., Luus, K. A., Chang, R. Y.-W., Daube, B. C., et al. (2017). Carbon dioxide sources from Alaska driven by increasing early winter respiration from Arctic tundra. *Proceedings of the National Academy of Sciences*, *114*(21), 5361–5366. https://doi.org/10.1073/pnas.1618567114

Cornelissen, J. H. C., Van Bodegom, P. M., Aerts, R., Callaghan, T. V., Van Logtestijn, R. S. P., Alatalo, J., et al. (2007). Global negative vegetation feedback to climate warming responses of leaf litter decomposition rates in cold biomes. *Ecology Letters*, *10*(7), 619–627. https://doi.org/10.1111/j.1461-0248.2007.01051.x

Dee, D. P., Uppala, S. M., Simmons, A. J., Berrisford, P., Poli, P., Kobayashi, S., et al. (2011). The ERA-Interim reanalysis: Configuration and performance of the data assimilation system. *Quarterly Journal of the Royal Meteorological Society*, *137*(656), 553–597. https://doi.org/10.1002/qj.828

DeMarco, J., Mack, M. C., & Bret-Harte, M. S. (2014). Effects of arctic shrub expansion on biophysical vs. biogeochemical drivers of litter decomposition. *Ecology*, *95*(7), 1861–1875. https://doi.org/10.1890/13-2221.1

Dopheide, E., van der Meer, F., Sliuzas, R., van der Veen, A., & Voinov, A. (2012). *System Earth: Some theory on the system The core of GIScience: A systems-based approach. Enschede*. The Netherlands: The International Institute for Geo-Information Science and Earth Observation (ITC).

Essery, R. (2015). A factorial snowpack model (FSM 1.0). *Geoscientific Model Development*, *8*(12), 3867–3876. https://doi.org/10.5194/gmd-8-3867-2015

Euskirchen, E. S., Bret-Harte, M. S., Scott, G. J., Edgar, C., & Shaver, G. R. (2012). Seasonal patterns of carbon dioxide and water fluxes in three representative tundra ecosystems in northern Alaska. *Ecosphere*, *3*(1), 1–19. https://doi.org/10.1890/ES11-00202.1

Falge, E., Baldocchi, D., Olson, R., Anthoni, P., Aubinet, M., Bernhofer, C., et al. (2001). Gap filling strategies for defensible annual sums of net ecosystem exchange. *Agricultural and Forest Meteorology*, *107*(1), 43–69. https://doi.org/10.1016/S0168-1923(00)00225-2

Farquhar, G. D., & von Caemmerer, S. (1982). Modelling of photosynthetic response to environmental conditions. In O. L. Lange, P. S. Nobel, C. B. Osmond, & H. Ziegler (Eds.), *Physiological plant ecology II: Water relations and carbon assimilation* (pp. 549–587). Berlin, Heidelberg: Springer.

Goetz, S. J., Bunn, A. G., Fiske, G. J., & Houghton, R. A. (2005). Satellite-observed photosynthetic trends across boreal North America associated with climate and fire disturbance. *Proceedings of the National Academy of Sciences of the United States of America*, *102*(38), 13521–13525. https://doi.org/10.1073/pnas.0506179102

Groendahl, L., Friborg, T., & Soegaard, H. (2007). Temperature and snow-melt controls on interannual variability in carbon exchange in the high Arctic. *Theoretical and Applied Climatology*, *88*(1-2), 111–125. https://doi.org/10.1007/s00704-005-0228-y

Grøndahl, L., Friborg, T., Christensen, T. R., Ekberg, A., Elberling, B., Illeris, L., et al. (2008). In T. R. C. B. E. M. C. F, H. Meltofte, & R. Morten (Eds.), *Spatial and inter-annual variability of trace gas fluxes in a heterogeneous High-Arctic landscape*, *Advances in Ecological Research* (Vol. 40, pp. 473–498). London, UK: Academic Press.

Hanis, K. L., Amiro, B. D., Tenuta, M., Papakyriakou, T., & Swystun, K. A. (2015). Carbon exchange over four growing seasons for a subarctic sedge fen in northern Manitoba, Canada. *Arctic Science*, *1*(2), 27–44. https://doi.org/10.1139/as-2015-0003

Helfter, C., Campbell, C., Dinsmore, K. J., Drewer, J., Coyle, M., Anderson, M., et al. (2015). Drivers of long-term variability in CO_2 net ecosystem exchange in a temperate peatland. *Biogeosciences*, *12*(6), 1799–1811. https://doi.org/10.5194/bg-12-1799-2015

Heliasz, M., Johansson, T., Lindroth, A., Mölder, M., Mastepanov, M., Friborg, T., et al. (2011). Quantification of C uptake in subarctic birch forest after setback by an extreme insect outbreak. *Geophysical Research Letters*, *38*, L01704. https://doi.org/10.1029/2010GL044733

Hobbie, S. E., Schimel, J. P., Trumbore, S. E., & Randerson, J. R. (2000). Controls over carbon storage and turnover in high-latitude soils. *Global Change Biology*, *6*(S1), 196–210. https://doi.org/10.1046/j.1365-2486.2000.06021.x

Hopkins, F., Gonzalez-Meler, M. A., Flower, C. E., Lynch, D. J., Czimczik, C., Tang, J., & Subke, J.-A. (2013). Ecosystem-level controls on root-rhizosphere respiration. *New Phytologist*, *199*(2), 339–351. https://doi.org/10.1111/nph.12271

Hugelius, G., Bockheim, J. G., Camill, P., Elberling, B., Grosse, G., Harden, J. W., et al. (2013). A new data set for estimating organic carbon storage to 3 m depth in soils of the northern circumpolar permafrost region. *Earth System Science Data*, *5*(2), 393–402. https://doi.org/10.5194/essd-5-393-2013

Hugelius, G., Strauss, J., Zubrzycki, S., Harden, J. W., Schuur, E. A. G., Ping, C. L., et al. (2014). Improved estimates show large circumpolar stocks of permafrost carbon while quantifying substantial uncertainty ranges and identifying remaining data gaps. *Biogeosciences Discussions*, *11*(3), 4771–4822. https://doi.org/10.5194/bgd-11-4771-2014

IPCC (2013). In T. F. Stocker, et al. (Eds.), *Climate Change 2013: The Physical Science Basis. Contribution of Working Group I to the Fifth Assessment Report of the Intergovernmental Panel on Climate Change*. Cambridge, United Kingdom and New York, NY, USA: Cambridge University Press.

Jones, H. G. (1992). *Plants and microclimate*. Cambridge: Cambridge University Press.

Kaiser, S., Göckede, M., Castro-Morales, K., Knoblauch, C., Ekici, A., Kleinen, T., et al. (2017). Process-based modelling of the methane balance in periglacial landscapes (JSBACH-methane). *Geoscientific Model Development*, *10*(1), 333–358. https://doi.org/10.5194/gmd-10-333-2017

Keenan, T. F., Darby, B., Felts, E., Sonnentag, O., Friedl, M. A., Hufkens, K., et al. (2014). Tracking forest phenology and seasonal physiology using digital repeat photography: A critical assessment. *Ecological Applications*, *24*(6), 1478–1489. https://doi.org/10.1890/13-0652.1

Koven, C. D., Ringeval, B., Friedlingstein, P., Ciais, P., Cadule, P., Khvorostyanov, D., et al. (2011). Permafrost carbon-climate feedbacks accelerate global warming. *Proceedings of the National Academy of Sciences*, *108*(36), 14769–14774. https://doi.org/10.1073/pnas.1103910108

Kwon, H.-J., Oechel, W. C., Zulueta, R. C., & Hastings, S. J. (2006). Effects of climate variability on carbon sequestration among adjacent wet sedge tundra and moist tussock tundra ecosystems. *Journal of Geophysical Research*, *111*, G03014. https://doi.org/10.1029/2005JG000036

Lafleur, P. M., Humphreys, E. R., St. Louis, V. L., Myklebust, M. C., Papakyriakou, T., Poissant, L., et al. (2012). Variation in peak growing season net ecosystem production across the Canadian Arctic. *Environmental Science & Technology*, *46*(15), 7971–7977. https://doi.org/10.1021/es300500m

Lasslop, G., Reichstein, M., Papale, D., Richardson, A. D., Arneth, A., Barr, A., et al. (2010). Separation of net ecosystem exchange into assimilation and respiration using a light response curve approach: critical issues and global evaluation. *Global Change Biology*, *16*(1), 187–208. https://doi.org/10.1111/j.1365-2486.2009.02041.x

López-Blanco, E., Lund, M., Williams, M., Tamstorf, M. P., Westergaard-Nielsen, A., Exbrayat, J. F., et al. (2017). Exchange of CO2 in Arctic tundra: Impacts of meteorological variations and biological disturbance. *Biogeosciences*, *14*(19), 4467–4483. https://doi.org/10.5194/bg-14-4467-2017

Lund, M., Falk, J. M., Friborg, T., Mbufong, H. N., Sigsgaard, C., Soegaard, H., & Tamstorf, M. P. (2012). Trends in CO_2 exchange in a high Arctic tundra heath, 2000-2010. *Journal of Geophysical Research*, *117*, G02001. https://doi.org/10.1029/2011JG001901

Lund, M., Raundrup, K., Westergaard-Nielsen, A., López-Blanco, E., Nymand, J., & Aastrup, P. (2017). Larval outbreaks in West Greenland: Instant and subsequent effects on tundra ecosystem productivity and CO(2) exchange. *Ambio*, *46*(Suppl 1), 26–38. https://doi.org/10.1007/s13280-016-0863-9

Mastepanov, M., Sigsgaard, C., Dlugokencky, E. J., Houweling, S., Strom, L., Tamstorf, M. P., & Christensen, T. R. (2008). Large tundra methane burst during onset of freezing. *Nature*, *456*(7222), 628–630. https://doi.org/10.1038/nature07464

Mastepanov, M., Sigsgaard, C., Tagesson, T., Ström, L., Tamstorf, M. P., Lund, M., & Christensen, T. R. (2012). Revisiting factors controlling methane emissions from high-arctic tundra. *Biogeosciences Discussions*, *9*(11), 15853–15900. https://doi.org/10.5194/bgd-9-15853-2012

McGuire, A. D., Anderson, L. G., Christensen, T. R., Dallimore, S., Guo, L., Hayes, D. J., et al. (2009). Sensitivity of the carbon cycle in the Arctic to climate change. *Ecological Monographs*, *79*(4), 523–555. https://doi.org/10.1890/08-2025.1

McGuire, A. D., Christensen, T. R., Hayes, D., Heroult, A., Euskirchen, E., Kimball, J. S., et al. (2012). An assessment of the carbon balance of Arctic tundra: comparisons among observations, process models, and atmospheric inversions. *Biogeosciences*, *9*(8), 3185–3204. https://doi.org/10.5194/bg-9-3185-2012

McGuire, A. D., Melillo, J. M., Randerson, J. T., Parton, W. J., Heimann, M., Meier, R. A., et al. (2000). Modeling the effects of snowpack on heterotrophic respiration across northern temperate and high latitude regions: Comparison with measurements of atmospheric carbon dioxide in high latitudes. *Biogeochemistry*, *48*(1), 91–114. https://doi.org/10.1023/a:1006286804351

Meltofte, H., Christensen, T. R., Elberling, B., Forchhammer, M. C., & Rasch, M. (2008). Introduction. In T. R. C. B. E. M. C. F, H. Meltofte, & R. Morten (Eds.), *Advances in ecological research* (Vol. 40, pp. 1–12). London, UK: Academic Press.

Moffat, A. M., Papale, D., Reichstein, M., Hollinger, D. Y., Richardson, A. D., Barr, A. G., et al. (2007). Comprehensive comparison of gap-filling techniques for eddy covariance net carbon fluxes. *Agricultural and Forest Meteorology*, *147*(3–4), 209–232. https://doi.org/10.1016/j.agrformet. 2007.08.011

Myers-Smith, I. H., Elmendorf, S. C., Beck, P. S. A., Wilmking, M., Hallinger, M., Blok, D., et al. (2015). Climate sensitivity of shrub growth across the tundra biome. *Nature Climate Change*, *5*, 887. https://doi.org/10.1038/nclimate2697

Oechel, W. C., Vourlitis, G., & Hastings, S. J. (1997). Cold season CO2 emission from Arctic soils. *Global Biogeochemical Cycles*, *11*(2), 163–172. https://doi.org/10.1029/96GB03035

Olefeldt, D., & Roulet, N. T. (2012). Effects of permafrost and hydrology on the composition and transport of dissolved organic carbon in a subarctic peatland complex. *Journal of Geophysical Research*, *117*, G01005. https://doi.org/10.1029/2011JG001819

Olefeldt, D., Roulet, N. T., Bergeron, O., Crill, P., Bäckstrand, K., & Christensen, T. R. (2012). Net carbon accumulation of a high-latitude permafrost palsa mire similar to permafrost-free peatlands. *Geophysical Research Letters*, *39*, L03501. https://doi.org/10.1029/2011GL050355

Papale, D., Reichstein, M., Aubinet, M., Canfora, E., Bernhofer, C., Kutsch, W., et al. (2006). Towards a standardized processing of Net Ecosystem Exchange measured with eddy covariance technique: Algorithms and uncertainty estimation. *Biogeosciences*, *3*(4), 571–583. https://doi.org/10.5194/bg-3-571-2006

Pirk, N., Mastepanov, M., López-Blanco, E., Christensen, L. H., Christiansen, H. H., Hansen, B. U., et al. (2017). Toward a statistical description of methane emissions from arctic wetlands. *Ambio*, *46*(1), 70–80. https://doi.org/10.1007/s13280-016-0893-3

Pirk, N., Tamstorf, M. P., Lund, M., Mastepanov, M., Pedersen, S. H., Mylius, M. R., et al. (2016). Snowpack fluxes of methane and carbon dioxide from high Arctic tundra. *Journal of Geophysical Research: Biogeosciences*, *121*, 2886–2900. https://doi.org/10.1002/2016JG003486

Poyatos, R., Heinemeyer, A., Ineson, P., Evans, J. G., Ward, H. C., Huntley, B., & Baxter, R. (2013). Environmental and vegetation drivers of seasonal CO2 fluxes in a sub-arctic forest–mire ecotone. *Ecosystems*, *17*(3), 377–393. https://doi.org/10.1007/s10021-013-9728-2

Rasmussen, L. H., Zhang, W., Hollesen, J., Cable, S., Christiansen, H. H., Jansson, P.-E., & Elberling, B. (2017). Modelling present and future permafrost thermal regimes in Northeast Greenland. *Cold Regions Science and Technology*. https://doi.org/10.1016/j.coldregions.2017.10.011

Reich, P. B., Tjoelker, M. G., Pregitzer, K. S., Wright, I. J., Oleksyn, J., & Machado, J.-L. (2008). Scaling of respiration to nitrogen in leaves, stems and roots of higher land plants. *Ecology Letters*, *11*(8), 793–801. https://doi.org/10.1111/j.1461-0248.2008.01185.x

Reichstein, M., Bahn, M., Mahecha, M. D., Kattge, J., & Baldocchi, D. D. (2014). Linking plant and ecosystem functional biogeography. *Proceedings of the National Academy of Sciences*, *111*(38), 13697–13702. https://doi.org/10.1073/pnas.1216065111

Reichstein, M., Falge, E., Baldocchi, D., Papale, D., Aubinet, M., Berbigier, P., et al. (2005). On the separation of net ecosystem exchange into assimilation and ecosystem respiration: Review and improved algorithm. *Global Change Biology*, *11*(9), 1424–1439. https://doi.org/10.1111/j.1365-2486.2005.001002.x

Riseborough, D., Shiklomanov, N., Etzelmüller, B., Gruber, S., & Marchenko, S. (2008). Recent advances in permafrost modelling. *Permafrost and Periglacial Processes*, *19*(2), 137–156. https://doi.org/10.1002/ppp.615

Rocha, A. V., & Shaver, G. R. (2011). Burn severity influences postfire CO2 exchange in arctic tundra. *Ecological Applications*, *21*(2), 477–489. https://doi.org/10.1890/10-0255.1

Rogers, A., Serbin, S. P., Ely, K. S., Sloan, V. L., & Wullschleger, S. D. (2017). Terrestrial biosphere models underestimate photosynthetic capacity and CO2 assimilation in the Arctic. *New Phytologist*, *216*(4), 1090–1103. https://doi.org/10.1111/nph.14740

Roulet, N. T., Lafleur, P. M., Richard, P. J. H., Moore, T. R., Humphreys, E. R., & Bubier, J. (2007). Contemporary carbon balance and late Holocene carbon accumulation in a northern peatland. *Global Change Biology*, *13*(2), 397–411. https://doi.org/10.1111/j.1365-2486.2006.01292.x

Schimel, J. P., & Clein, J. S. (1995). Microbial response to freeze-thaw cycles in tundra and taiga soils. *Soil Biology and Biochemistry*, *28*(8), 1061–1066. https://doi.org/10.1016/0038-0717(96)00083-1

Schneider, C. A., Rasband, W. S., & Eliceiri, K. W. (2012). NIH Image to ImageJ: 25 years of Image Analysis. *Nature Methods*, *9*(7), 671–675.

Schuur, E. A. G., McGuire, A. D., Schadel, C., Grosse, G., Harden, J. W., Hayes, D. J., et al. (2015). Climate change and the permafrost carbon feedback. *Nature*, *520*(7546), 171–179. https://doi.org/10.1038/nature14338

Serreze, M. C., & Barry, R. G. (2011). Processes and impacts of Arctic amplification: A research synthesis. *Global and Planetary Change*, *77*(1–2), 85–96. https://doi.org/10.1016/j.gloplacha.2011.03.004

Shulski, M., & Wendler, G. (2007). *The Climate of Alaska* (216 pp). Fairbanks, AK: University of Alaska Press, Snowy Owl Books.

Sloan, V. L., Fletcher, B. J., Press, M. C., Williams, M., & Phoenix, G. K. (2013). Leaf and fine root carbon stocks and turnover are coupled across Arctic ecosystems. *Global Change Biology*, *19*(12), 3668–3676. https://doi.org/10.1111/gcb.12322

Smallman, T. L., Moncrieff, J. B., & Williams, M. (2013). WRFv3.2-SPAv2: development and validation of a coupled ecosystem–atmosphere model, scaling from surface fluxes of CO2 and energy to atmospheric profiles. *Geoscientific Model Development*, *6*(4), 1079–1093. https://doi.org/10.5194/gmd-6-1079-2013

Street, L. E., Shaver, G. R., Rastetter, E. B., van Wijk, M. T., Kaye, B. A., & Williams, M. (2012). Incident radiation and the allocation of nitrogen within Arctic plant canopies: Implications for predicting gross primary productivity. *Global Change Biology*, *18*(9), 2838–2852. https://doi.org/10.1111/j.1365-2486.2012.02754.x

Street, L. E., Stoy, P. C., Sommerkorn, M., Fletcher, B. J., Sloan, V. L., Hill, T. C., & Williams, M. (2012). Seasonal bryophyte productivity in the sub-Arctic: A comparison with vascular plants. *Functional Ecology*, *26*(2), 365–378. https://doi.org/10.1111/j.1365-2435.2011.01954.x

Street, L. E., Subke, J.-A., Sommerkorn, M., Sloan, V., Ducrotoy, H., Phoenix, G. K., & Williams, M. (2013). The role of mosses in carbon uptake and partitioning in arctic vegetation. *New Phytologist*, *199*(1), 163–175. https://doi.org/10.1111/nph.12285

Tagesson, T., Mölder, M., Mastepanov, M., Sigsgaard, C., Tamstorf, M. P., Lund, M., et al. (2012). Land-atmosphere exchange of methane from soil thawing to soil freezing in a high-Arctic wet tundra ecosystem. *Global Change Biology*, *18*(6), 1928–1940. https://doi.org/10.1111/j.1365-2486.2012.02647.x

Tarnocai, C., Canadell, J. G., Schuur, E. A. G., Kuhry, P., Mazhitova, G., & Zimov, S. (2009). Soil organic carbon pools in the northern circumpolar permafrost region. *Global Biogeochemical Cycles*, *23*, GB2023. https://doi.org/10.1029/2008GB003327

Thornton, P. E., & Rosenbloom, N. A. (2005). Ecosystem model spin-up: Estimating steady state conditions in a coupled terrestrial carbon and nitrogen cycle model. *Ecological Modelling*, *189*(1), 25–48. https://doi.org/10.1016/j.ecolmodel.2005.04.008

Tjoelker, M. G., Oleksyn, J., & Reich, P. B. (2001). Modelling respiration of vegetation: Evidence for a general temperature-dependent Q10. *Global Change Biology*, *7*(2), 223–230. https://doi.org/10.1046/j.1365-2486.2001.00397.x

Uchida, M., Muraoka, H., & Nakatsubo, T. (2016). Sensitivity analysis of ecosystem CO2 exchange to climate change in High Arctic tundra using an ecological process-based model. *Polar Biology*, *39*(2), 251–265. https://doi.org/10.1007/s00300-015-1777-x

van der Kolk, H. J., Heijmans, M. M. P. D., van Huissteden, J., Pullens, J. W. M., & Berendse, F. (2016). Potential Arctic tundra vegetation shifts in response to changing temperature, precipitation and permafrost thaw. *Biogeosciences*, *13*(22), 6229–6245. https://doi.org/10.5194/bg-13-6229-2016

van der Molen, M. K., van Huissteden, J., Parmentier, F. J. W., Petrescu, A. M. R., Dolman, A. J., Maximov, T. C., et al. (2007). The growing season greenhouse gas balance of a continental tundra site in the Indigirka lowlands, NE Siberia. *Biogeosciences*, *4*(6), 985–1003. https://doi.org/10.5194/bg-4-985-2007

Van Wijk, M. T., Clemmensen, K. E., Shaver, G. R., Williams, M., Callaghan, T. V., Chapin, F. S., et al. (2004). Long-term ecosystem level experiments at Toolik Lake, Alaska, and at Abisko, Northern Sweden: generalizations and differences in ecosystem and plant type responses to global change. *Global Change Biology*, *10*(1), 105–123. https://doi.org/10.1111/j.1365-2486.2003.00719.x

Walter, B. P., & Heimann, M. (2000). A process-based, climate-sensitive model to derive methane emissions from natural wetlands: Application to five wetland sites, sensitivity to model parameters, and climate. *Global Biogeochemical Cycles*, *14*(3), 745–765. https://doi.org/10.1029/1999GB001204

Walter, B. P., Heimann, M., & Matthews, E. (2001). Modeling modern methane emissions from natural wetlands: 1. Model description and results. *Journal of Geophysical Research*, *106*(D24), 34189–34206. https://doi.org/10.1029/2001JD900165

Waring, R. H., & Schlesinger, W. H. (1985). *Forest ecosystems: concepts and management*. London, UK: Academic Press.

Webb, E. E., Schuur, E. A. G., Natali, S. M., Oken, K. L., Bracho, R., Krapek, J. P., et al. (2016). Increased wintertime CO2 loss as a result of sustained tundra warming. *Journal of Geophysical Research: Biogeosciences*, *121*, 249–265. https://doi.org/10.1002/2014JG002795

Westergaard-Nielsen, A., Lund, M., Hansen, B. U., & Tamstorf, M. (2013). Camera derived vegetation greenness index as proxy for gross primary production in a low Arctic wetland area. *ISPRS Journal of Photogrammetry and Remote Sensing*, *86*, 89–99. https://doi.org/10.1016/j.isprsjprs.2013.09.006

Westergaard-Nielsen, A., Lund, M., Pedersen, S. H., Schmidt, N. M., Klosterman, S., Abermann, J., & Hansen, B. U. (2017). Transitions in high-Arctic vegetation growth patterns and ecosystem productivity tracked with automated cameras from 2000 to 2013. *Ambio*, *46*(1), 39–52. https://doi.org/10.1007/s13280-016-0864-8

Williams, M., Eugster, W., Rastetter, E. B., McFadden, J. P., & Chapin, F. S. III (2000). The controls on net ecosystem productivity along an Arctic transect: a model comparison with flux measurements. *Global Change Biology*, *6*(S1), 116–126. https://doi.org/10.1046/j.1365-2486.2000.06016.x

Williams, M., Law, B. E., Anthoni, P. M., & Unsworth, M. H. (2001). Use of a simulation model and ecosystem flux data to examine carbon-water interactions in ponderosa pine. *Tree Physiology*, *21*(5), 287–298.

Williams, M., Malhi, Y., Nobre, A. D., Rastetter, E. B., Grace, J., & Pereira, M. G. P. (1998). Seasonal variation in net carbon exchange and evapotranspiration in a Brazilian rain forest: A modelling analysis. *Plant, Cell & Environment*, *21*(10), 953–968. https://doi.org/10.1046/j.1365-3040.1998.00339.x

Williams, M., & Rastetter, E. B. (1999). Vegetation characteristics and primary productivity along an arctic transect: Implications for scaling-up. *Journal of Ecology*, *87*(5), 885–898. https://doi.org/10.1046/j.1365-2745.1999.00404.x

Williams, M., Rastetter, E. B., Fernandes, D. N., Goulden, M. L., Wofsy, S. C., Shaver, G. R., et al. (1996). Modelling the soil-plant-atmosphere continuum in a Quercus–Acer stand at Harvard Forest: the regulation of stomatal conductance by light, nitrogen and soil/plant hydraulic properties. *Plant, Cell & Environment*, *19*(8), 911–927. https://doi.org/10.1111/j.1365-3040.1996.tb00456.x

Williams, M., Schwarz, P. A., Law, B. E., Irvine, J., & Kurpius, M. R. (2005). An improved analysis of forest carbon dynamics using data assimilation. *Global Change Biology*, *11*(1), 89–105. https://doi.org/10.1111/j.1365-2486.2004.00891.x

Zona, D., Gioli, B., Commane, R., Lindaas, J., Wofsy, S. C., Miller, C. E., et al. (2016). Cold season emissions dominate the Arctic tundra methane budget. *Proceedings of the National Academy of Sciences*, *113*(1), 40–45. https://doi.org/10.1073/pnas.1516017113